

Supporting Information

Arylsilylation of aryl halides using the magnetically recyclable bimetallic catalyst Pd–Pt–Fe₃O₄

Jisun Jang, †^a Sangmoon Byun, †^{b,c} B. Moon Kim,^{b,} Sunwoo Lee^{a,*}*

^a Department of Chemistry, Chonnam National University, 61186, Gwangju, Republic of Korea

^b Department of Chemistry, College of Natural Sciences, Seoul National University, 1 Gwanak-ro, Gwanak-gu, Seoul, 08826, Republic of Korea

^c The Research Institute of Basic Sciences, Seoul National University, 1 Gwanak-ro, Gwanak-gu, Seoul, 08826, Republic of Korea

† These authors contributed equally.

Corresponding author's email address: sunwoo@chonnam.ac.kr and
kimbm@snu.ac.kr

Materials/Instrumentation

ESCA (Electron Spectroscopy for Chemical Analysis)

1. Model: SIGMA PROBE (ThermoVG, U.K.)

X-ray source		Monochromatic Al-K (15 kV, 100W, 400 micrometer)
Wide scan	pass energy	50 eV
	step size	1.0 eV
Narrow scan	pass energy	20 eV
	step size	0.1 eV
Flood gun		off
Ion etching gun		off

Transmission Electron Microscope II (ccd camera type)

1. Model: JEM-2100
2. Accelerating Voltage: 80 to 200Kv
3. Gatan Digital Camera (ORIUS-SC600)
4. Resolution: Point image: 0.23nm
Lattice image: 0.14nm
5. MAG: x50 ~ x1 500 000
6. Camera Length: SA DIFF Mode: 80 ~ 2 000mm

Cs-STEM (Cs corrected STEM with Cold FEG)

1. Model: JEM-ARM200F (Cold Field Emission Type, JEOL)
2. Specifications
 - a. HT: 60, 80, 120, 200 kV
 - b. Magnification: 50 to 2,000,000 X (TEM), 200 to 1,500,000 X (STEM)
 - c. Resolution
 - STEM mode: HAADF 0.1nm/ BF 0.136nm
 - TEM mode: Point 0.23nm
 - d. Sample tilting
 - X / Y: ±35° / ±30°
3. Analysis functions
 - a. CCD Camera: UltraScan 1000XP (2,048 x 2,048 pixel)
 - b. EDS: SDD Type (Active area 100mm²/ Solid angle 0.9 str)
 - c. EELS: Model 965 GIF Quantum ER

Pd–Pt–Fe₃O₄ samples were analyzed on **ESCA**, **HR-TEM** and **Cs-STEM (Cs corrected STEM with Cold FEG)**, and **High resolution-Transmission Electron Microscope (ccd camera type)** installed at the **National Center for Inter-university Research Facilities (NCIRF) at Seoul National University**.

Synthesis of the Pd–Pt–Fe₃O₄

340 mg of palladium(II) chloride (PdCl₂), 800 mg of potassium platinochloride (K₂PtCl₄) and 4.00 g of polyvinylpyrrolidone (PVP) (Mw ~ 10,000) were put in 80 mL of ethylene glycol (EG) in a 250 mL round-bottom flask. This solution was sonicated for 10 min and heated for 1 h at 100°C with magnetic stirring. Meanwhile, 1.00 g of commercially available Fe₃O₄(DK-Nano) was added to 300 mL of EG in a two-necked 500 mL round-bottom flask. Then, the prepared solution was injected dropwise then stirred at 100°C for additional 24 h. The resultant product washed with ethanol. Finally, the product was obtained via drying on a rotary evaporator.

Synthesis of the Pd–Fe₃O₄

340 mg of palladium(II) chloride (PdCl₂) and 4.00 g of polyvinylpyrrolidone (PVP) (Mw ~ 10,000) were put in 80 mL of ethylene glycol (EG) in a 250 mL round-bottom flask. This solution was sonicated for 10 min and heated for 1 h at 100°C with magnetic stirring. Meanwhile, 1.00 g of commercially available Fe₃O₄(DK-Nano) was added to 300 mL of EG in a two-necked 500 mL round-bottom flask. Then, the prepared solution was injected dropwise then stirred at 100°C for additional 24 h. The resultant product washed with ethanol. Finally, the product was obtained via drying on a rotary evaporator.

Synthesis of the Pt–Fe₃O₄

400 mg of potassium platinochloride (K₂PtCl₄) and 0.50 g of polyvinylpyrrolidone (PVP) (Mw ~ 10,000) were put in 80 mL of ethylene glycol (EG) in a 250 mL round-bottom flask. This solution was sonicated for 10 min and heated for 1 h at 100°C with magnetic stirring. Meanwhile, 0.50 g of commercially available Fe₃O₄(DK-Nano) was added to 300 mL of EG in a two-necked 500 mL round-bottom flask. Then, the prepared solution was injected dropwise then stirred at 100°C for additional 24 h. The resultant product washed with ethanol. Finally, the product was obtained via drying on a rotary evaporator.

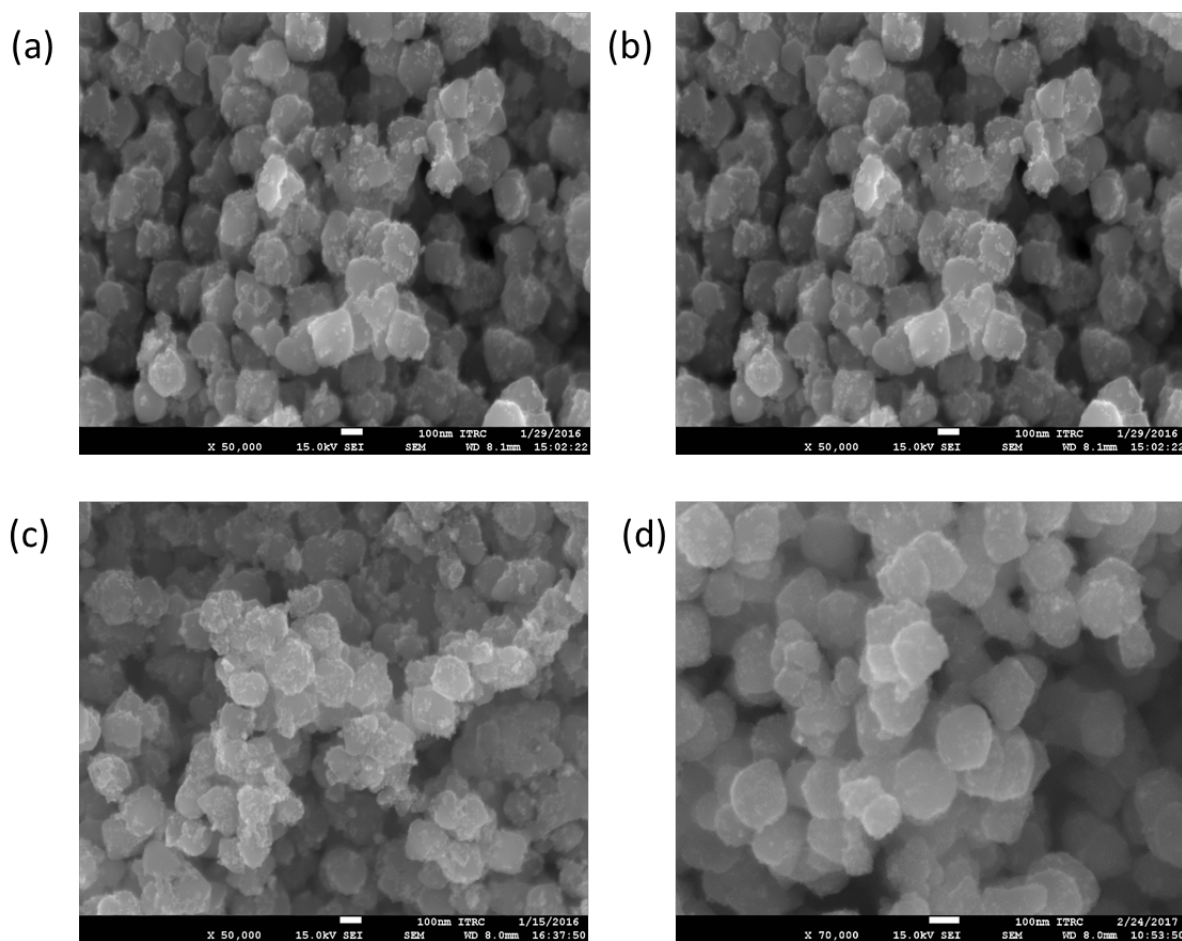


Fig. S1. SEM images of Pd–Pt– Fe_3O_4 NPs: (a) 1 eq of PVP used (1 g Fe_3O_4 NPs scale); (b) 2 eq of PVP used (1 g Fe_3O_4 NPs scale); (c) 3 eq of PVP used (1 g Fe_3O_4 NPs scale); (d) 4 eq of PVP used (1 g Fe_3O_4 NPs scale)

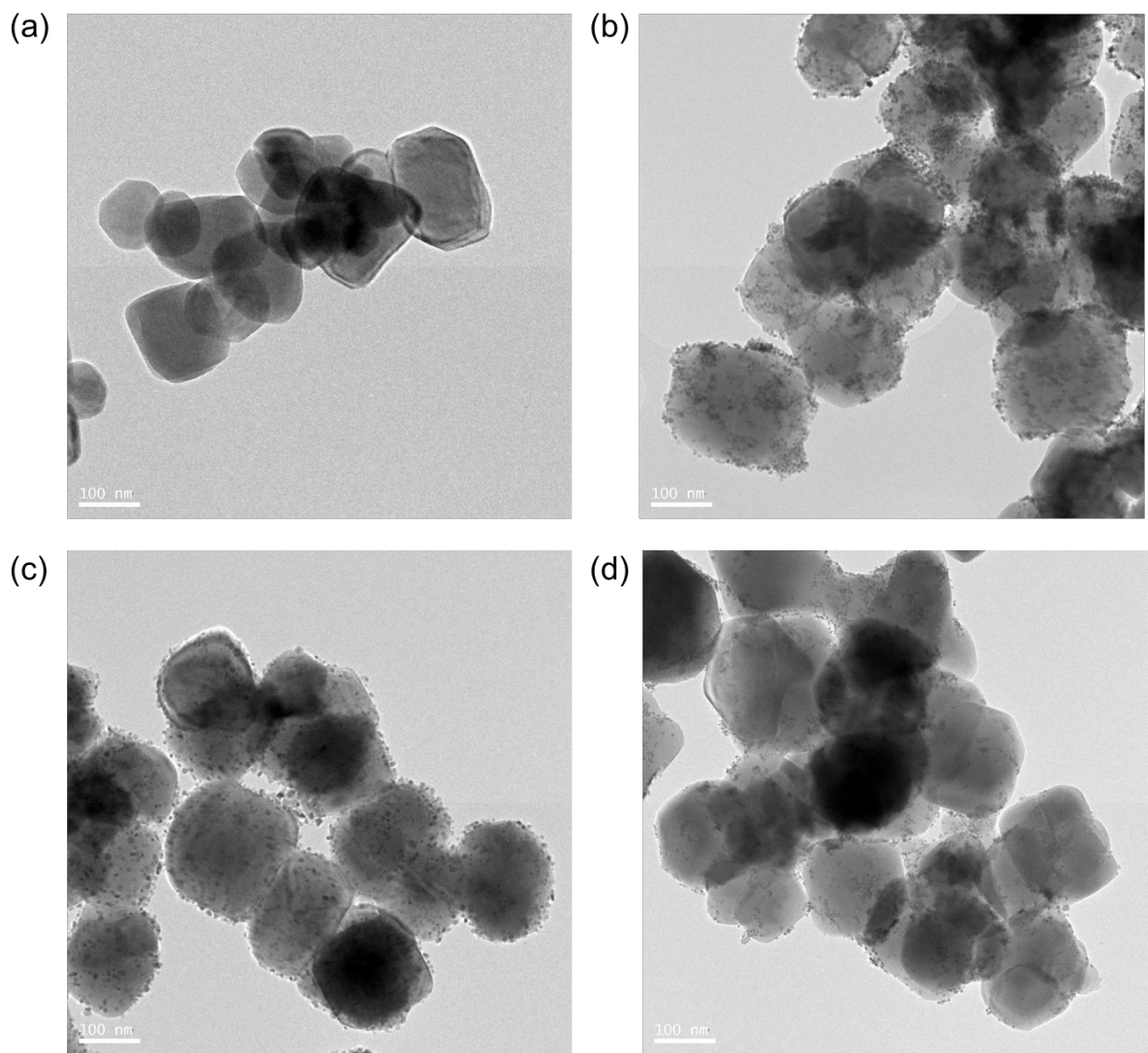


Fig. S2. HR-TEM images of fresh NPs: (a) Fe_3O_4 NPs; (b) Pd–Pt– Fe_3O_4 NPs; (c) Pd– Fe_3O_4 NPs; (d) Pt– Fe_3O_4 NPs.

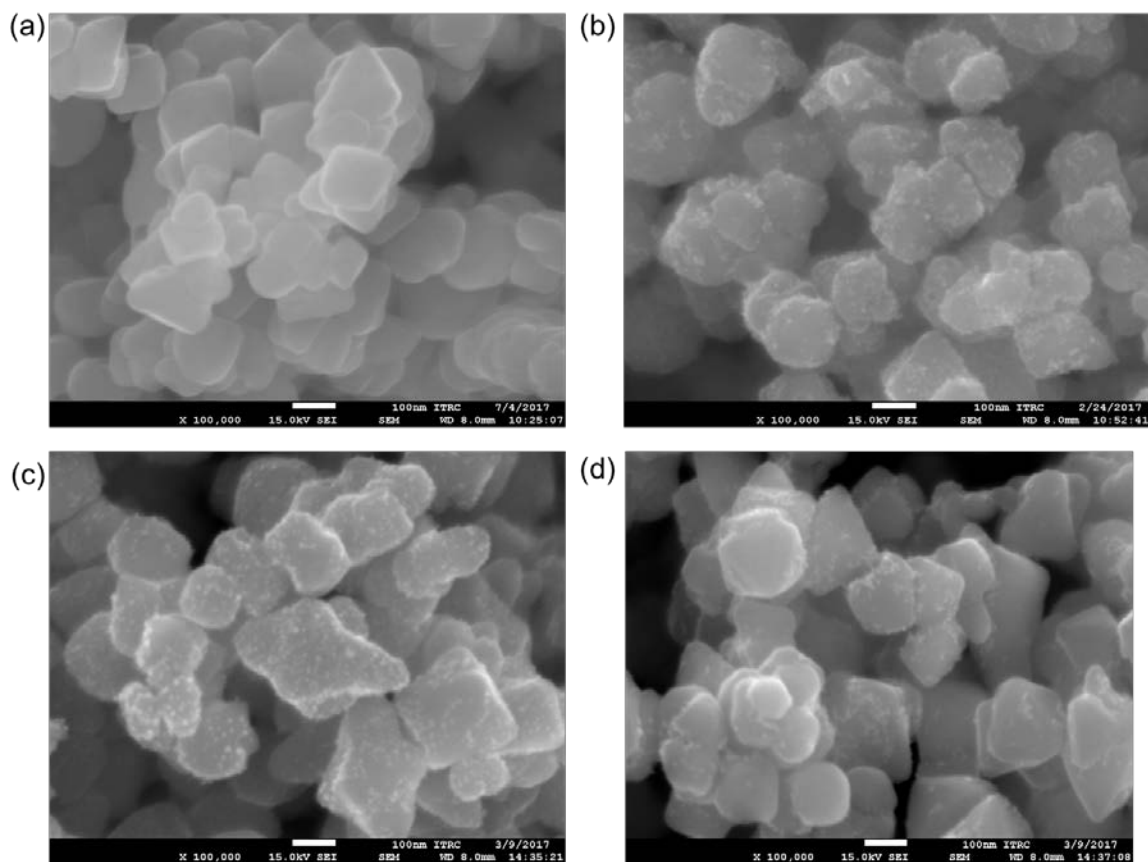


Fig. S3. SEM images of fresh NPs: (a) Fe_3O_4 NPs; (b) Pd–Pt– Fe_3O_4 NPs;
(c) Pd– Fe_3O_4 NPs; (d) Pt– Fe_3O_4 NPs

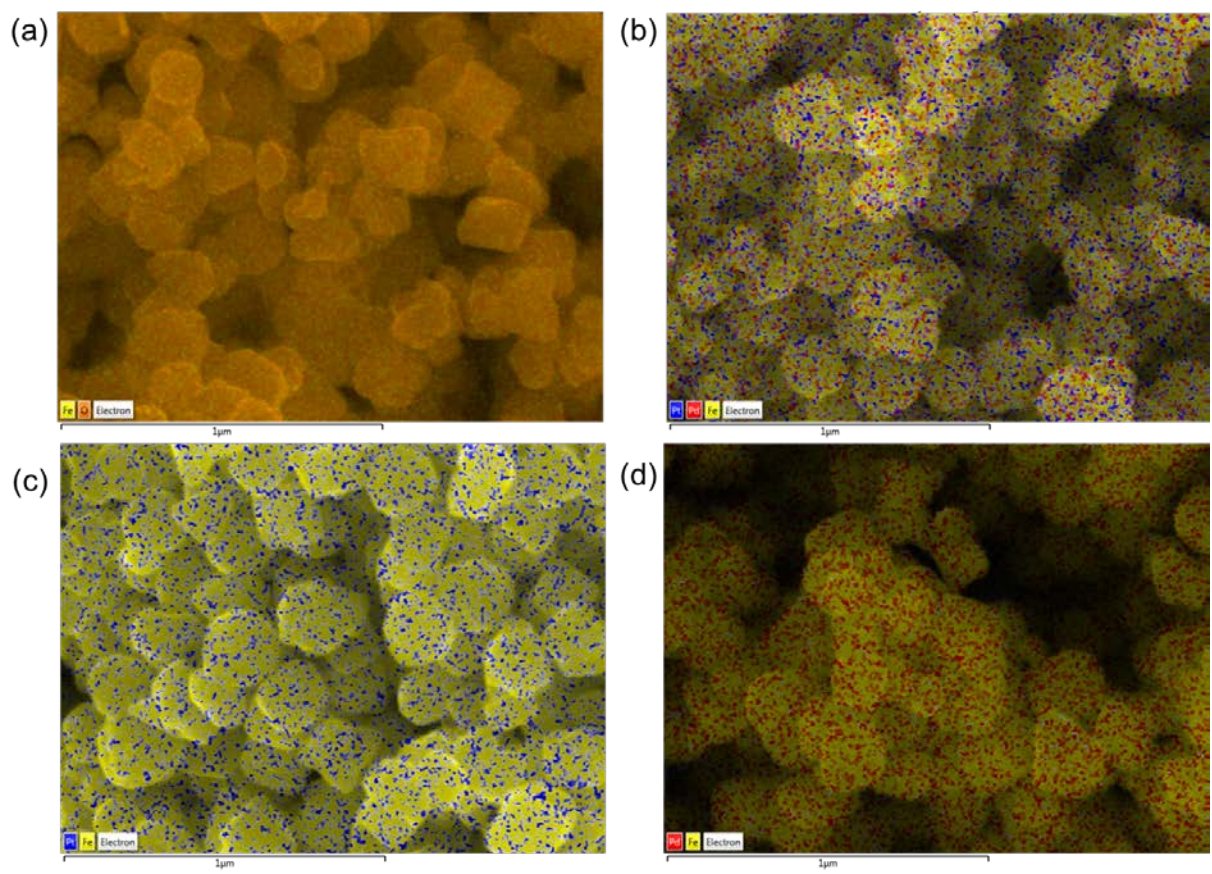


Fig. S4. The SEM-EDS mapping images of (a) Fe₃O₄ NPs, (b) Pd–Pt–Fe₃O₄ NPs, (c) Pd–Fe₃O₄ NPs and (d) Pt–Fe₃O₄ NPs.

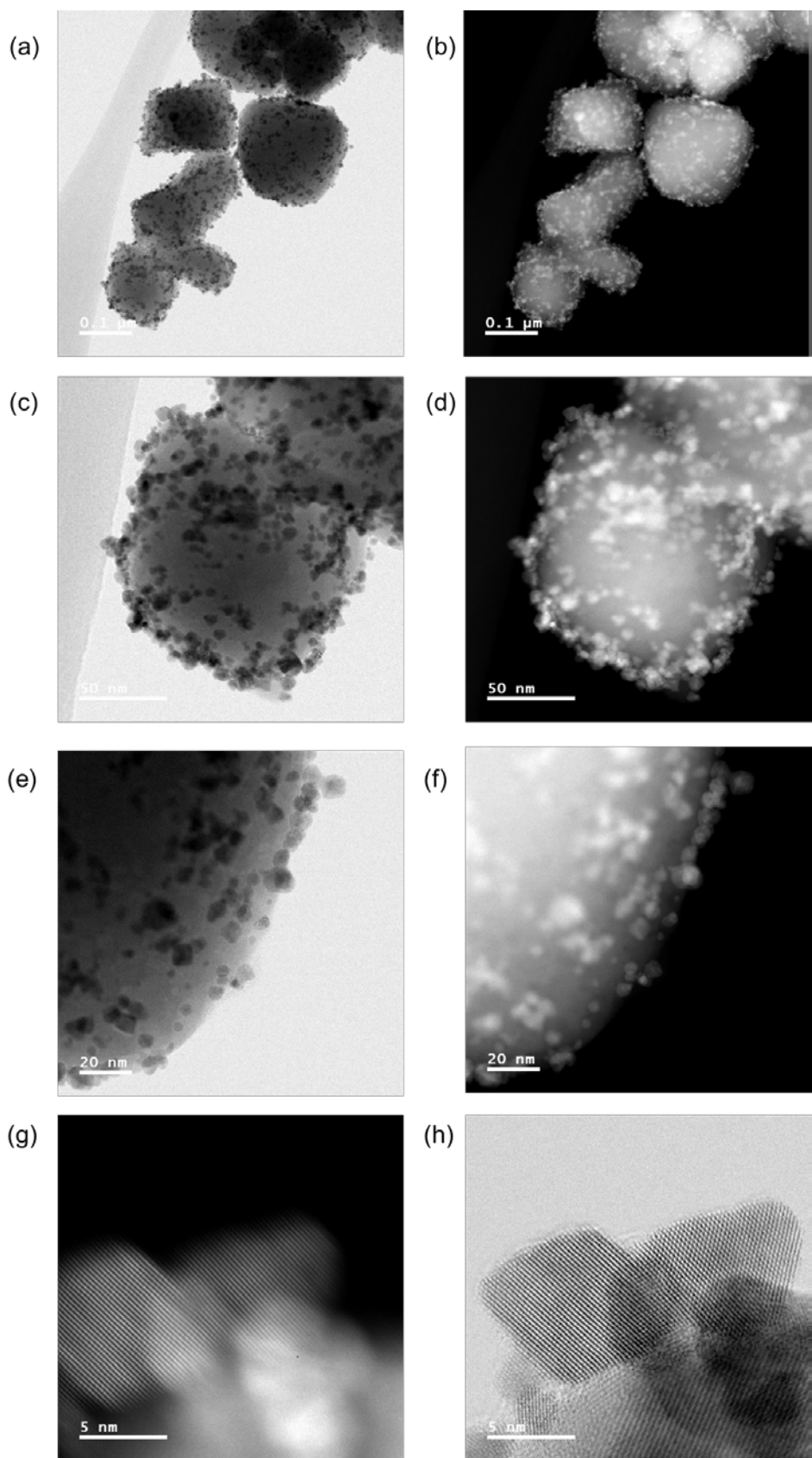


Fig. S5. (a) , (c), (e) and (g) BF-STEM image of image of Pd–Pt– Fe_3O_4 NPs; (b), (d), (f) and (h) HAADF-STEM image of image of Pd–Pt– Fe_3O_4 NPs

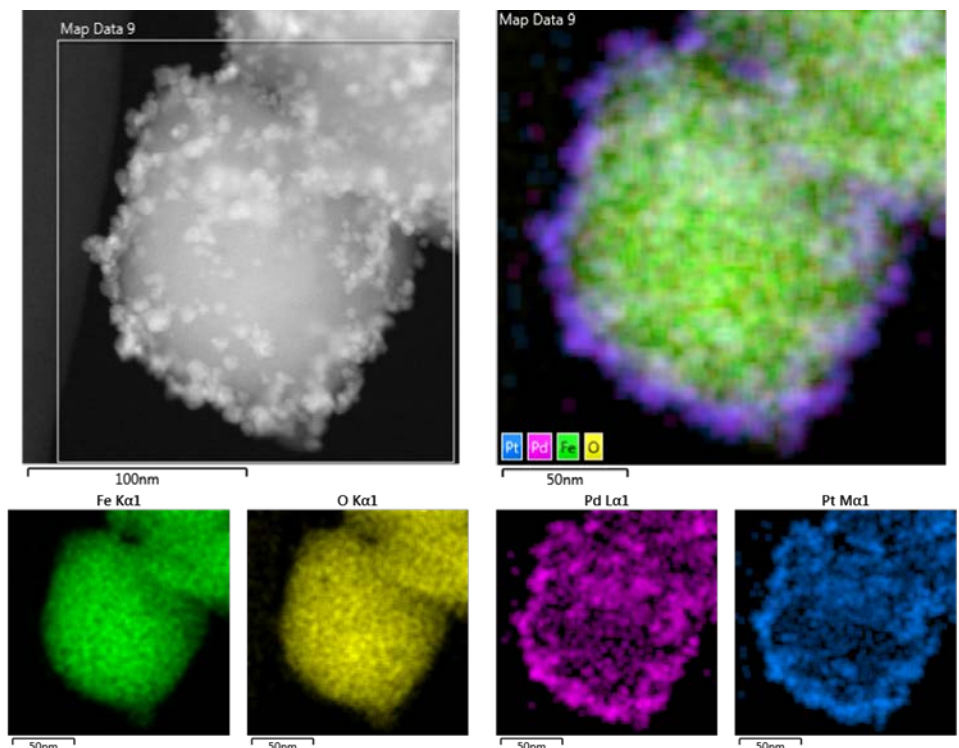


Fig. S6. The elemental analysis of Pd–Pt– Fe_3O_4 NPs mapping images by Cs-STEM-EDS

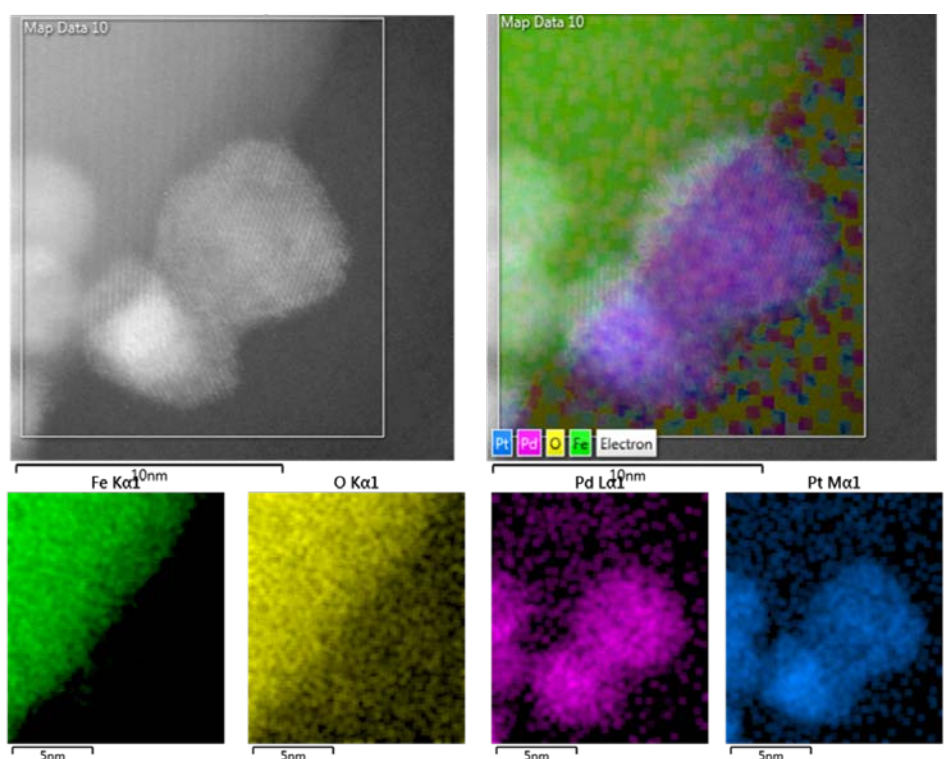


Fig. S7. The elemental analysis of loaded Pd–Pt alloy NPs mapping images by Cs-STEM-EDS

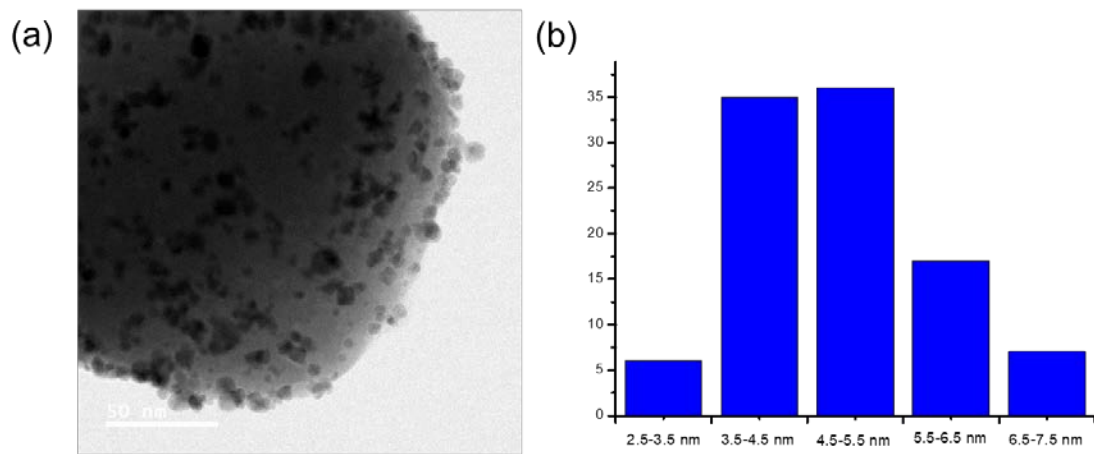


Fig. S8. The STEM and particle size distribution images of Pd–Pt–Fe₃O₄

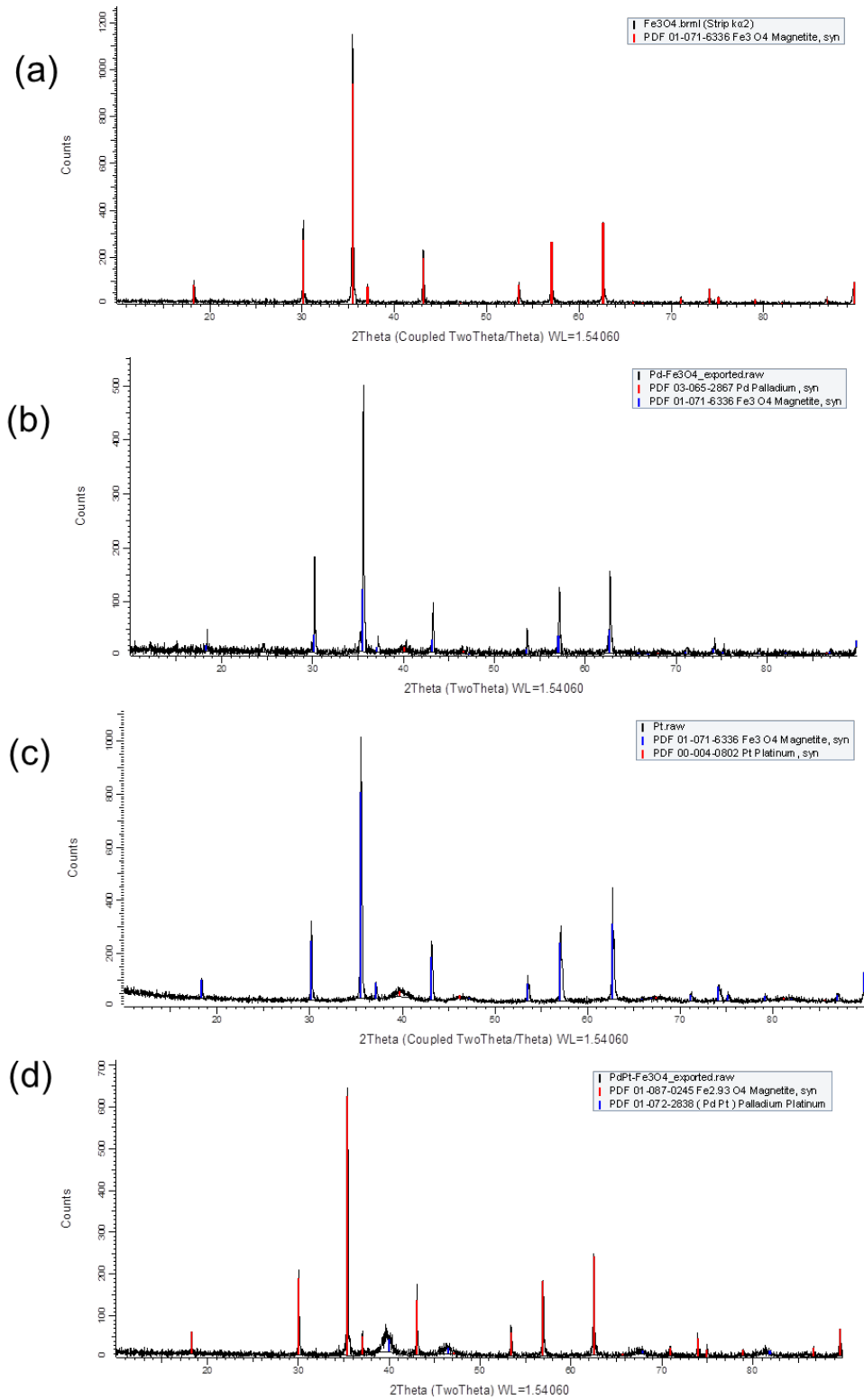


Fig. S9. The XRD data of (a) Fe_3O_4 NPs; (b) Pd– Fe_3O_4 NPs; (c) Pt– Fe_3O_4 NPs; (d) Pd–Pt– Fe_3O_4 NPs.

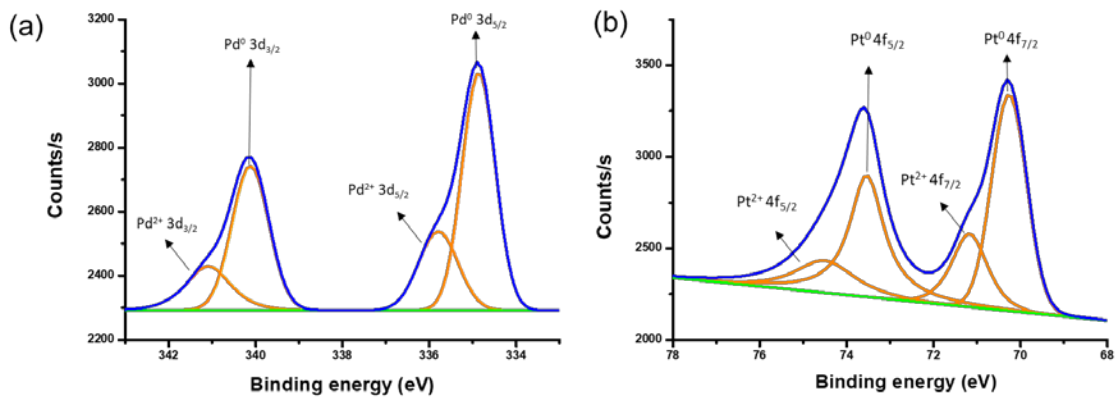


Fig. S10. The XPS data (a) Pd 4d peaks of Fresh Pd–Pt–Fe₃O₄ NPs (b) Pt 4f peaks of Fresh Pd–Pt–Fe₃O₄ NPs

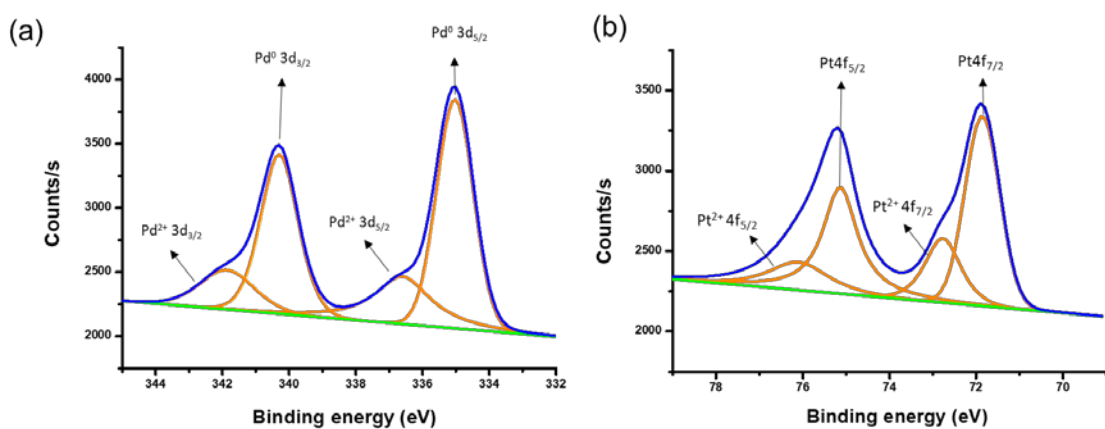


Fig. S11. The XPS data (a) Pd 4d peaks of fresh Pd–Fe₃O₄ (b) Pt 4f peaks of fresh Pt–Fe₃O₄ NPs

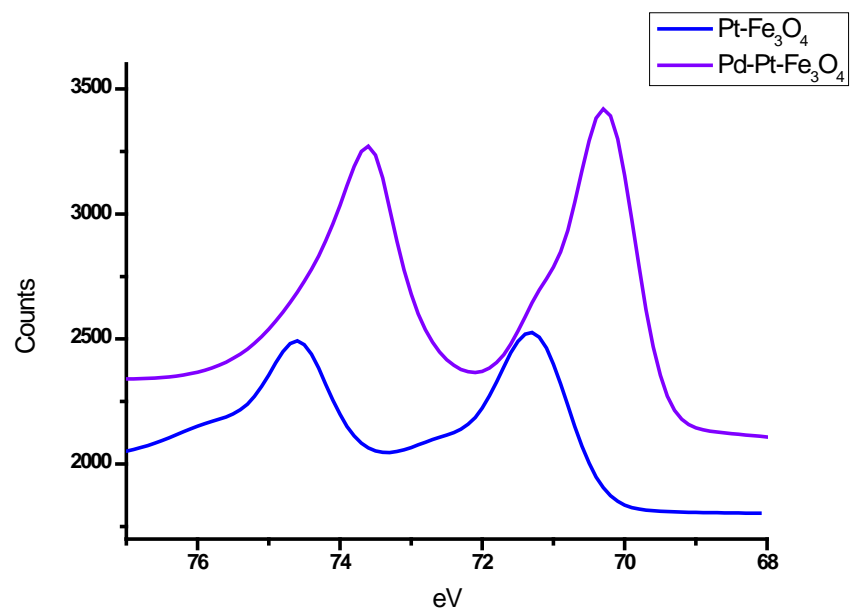


Fig. S12. The Pt XPS data of fresh Pt– Fe_3O_4 , and Pd–Pt– Fe_3O_4 NPs

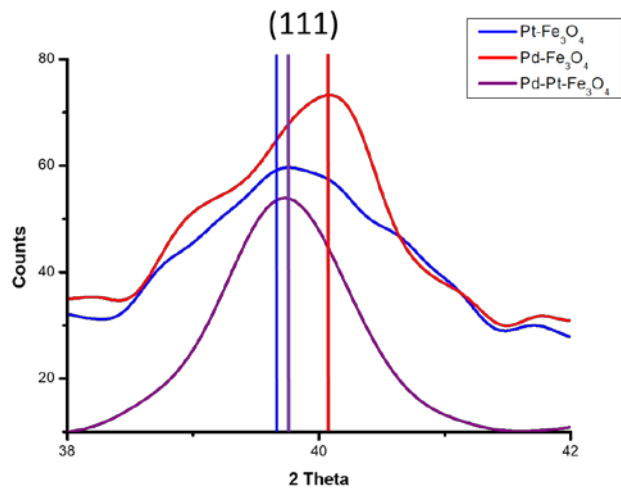


Fig. S13. The XRD (111) peak of Pd– Fe_3O_4 , Pt– Fe_3O_4 and Pd–Pt– Fe_3O_4 NPs

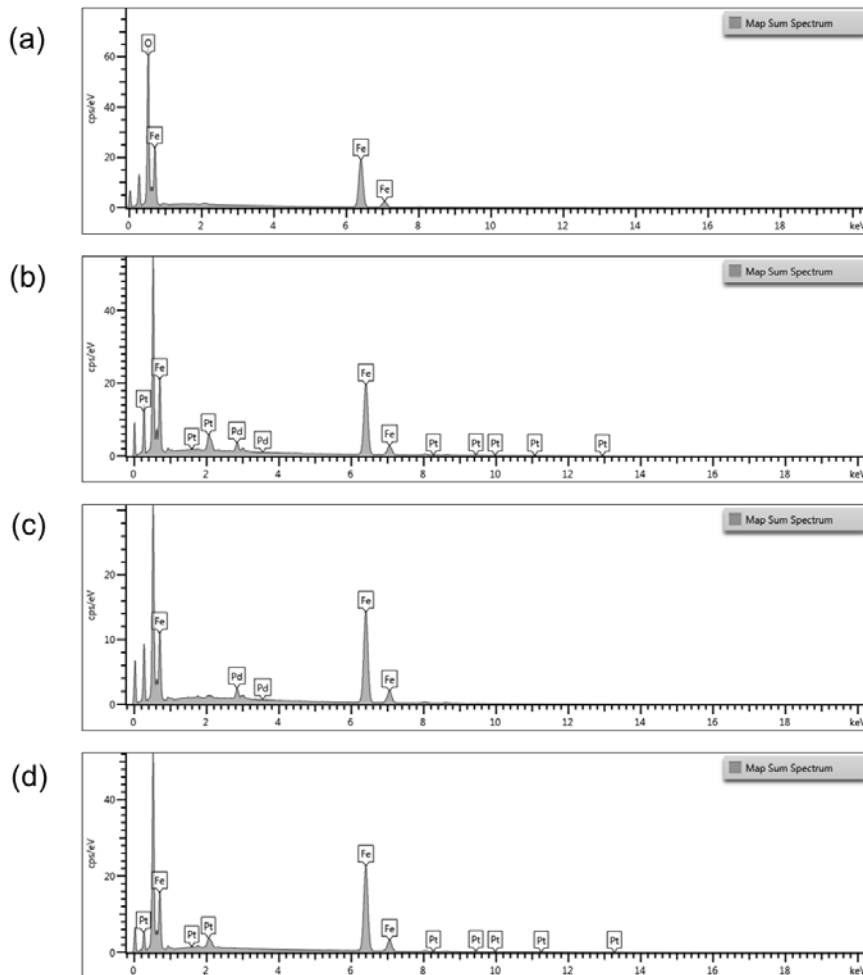


Fig. S14. The energy disperse spectroscopy (EDS) map sum spectrum pattern of NPs: (a) Fe_3O_4 NPs; (b) Pd–Pt– Fe_3O_4 NPs; (c) Pd– Fe_3O_4 NPs; (d) Pt– Fe_3O_4 NPs.

Explanation of XRD, XPS and EDS data

To confirm the detailed characterization of Pd–Pt– Fe_3O_4 NPs, X-ray photoelectron spectroscopy (XPS) and X-ray diffraction (XRD) were performed, and the results are shown in Fig. S8-S11. In Fig. S9, the characteristic peaks for major Pd^0 and minor Pd^{2+} can be seen, with the peaks $\text{Pd } 3\text{d}_{3/2}$ and $\text{Pd } 3\text{d}_{25/2}$, respectively.¹ Two Pt $4\text{f}_{5/2}$ and Pt $4\text{f}_{7/2}$ peaks were identified and these two binding energies in particular indicate Pt^0 and Pt^{2+} species.² The Pd–Pt– Fe_3O_4 XPS peaks were shifted to lower binding energy compared to monometallic Pd– or Pt– Fe_3O_4 , demonstrating the formation of the Pd–Pt alloy (Fig S9-10). As can be seen in Fig. S9, the X-ray diffraction (XRD) pattern of Pd–, Pt– and Pd–Pt– Fe_3O_4 NPs indicated the presence of all constituent elements in each NPs. The diffraction patterns of Pd– and Pt– Fe_3O_4 NPs in Pd(100) and Pt(100) could be clearly indexed as the platinum and palladium, respectively. A lattice peak change of Pd–Pt(100) was detected, which also indicates that the Pd–Pt NPs comprised a random alloy composition on Fe_3O_4 support (Fig. S13).³ We measured the energy dispersive spectroscopy (EDS) map sum spectrum pattern of Fe_3O_4 , Pd– Fe_3O_4 , Pt– Fe_3O_4 , and Pd–Pt– Fe_3O_4 . The presence of Pd, Pt, and Fe on Pd–Pt– Fe_3O_4 was clearly confirmed (Fig. S14).

1. (a) W. Yang, C. Yang, M. Sun, F. Yang, Y. Ma, Z. Zhang and X. Yang, *Talanta*, 2009, **78**, 557-564; (b) M. Peuckert and H. P. Bonzel, *Surf. Sci.*, 1984, **145**, 239-259.
2. K. S. Kim, A. F. Gossman and N. Winograd, *Anal. Chem.*, 2002, **46**, 197-200.
3. (a) S. Byun, Y. Song and B. M. Kim, *ACS Appl. Mater. Interfaces*, 2016, **8**, 14637-14647; (b) W. Wang, Q. Huang, J. Liu, Z. Zou, Z. Li and H. Yang, *Electrochim. Commun.*, 2008, **10**, 1396-1399.

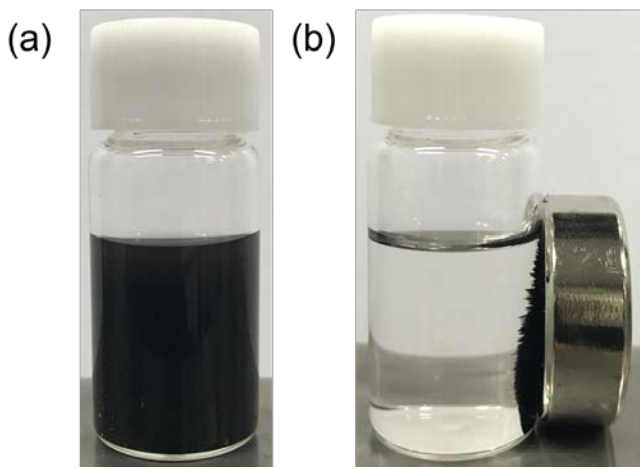


Fig. S15. Photographs of the magnetically separable Pd–Pt– Fe_3O_4 NPs: (a) dispersion state; (b) magnetic separation of Pd–Pt– Fe_3O_4 NPs.

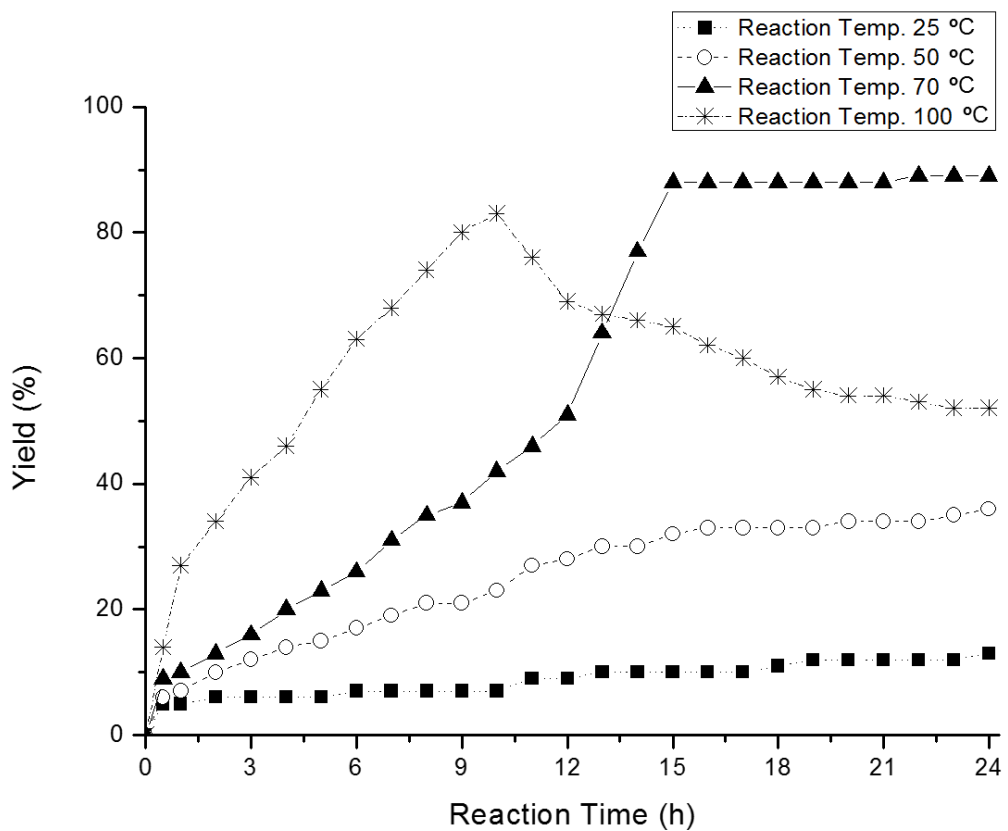


Fig. S16. Reaction yields at 25, 50, 70 and 100 °C.

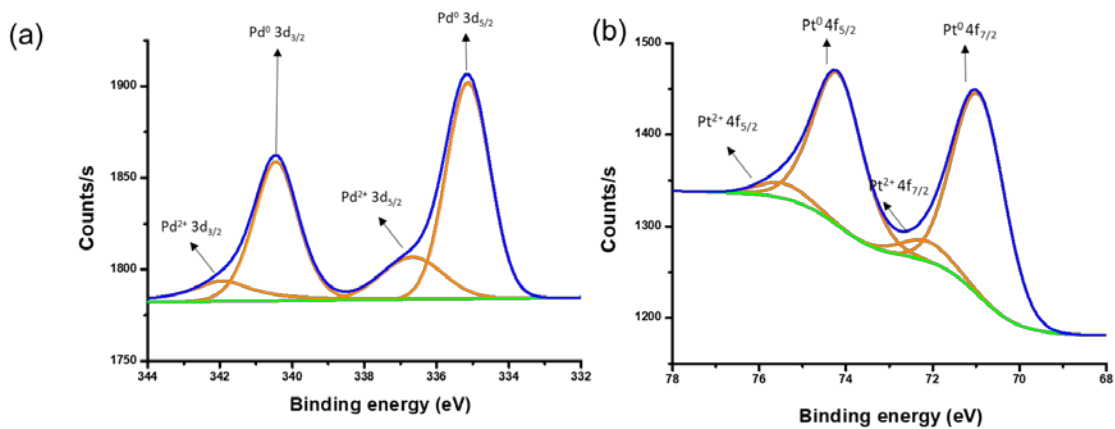


Fig. S17. The XPS data (a) Pd 4d peaks of Pd–Pt–Fe₃O₄ NPs after 20 cycle of the catalytic reactions (b) Pt 4f peaks of Pd–Pt–Fe₃O₄ NPs after 20 cycle of the catalytic reactions

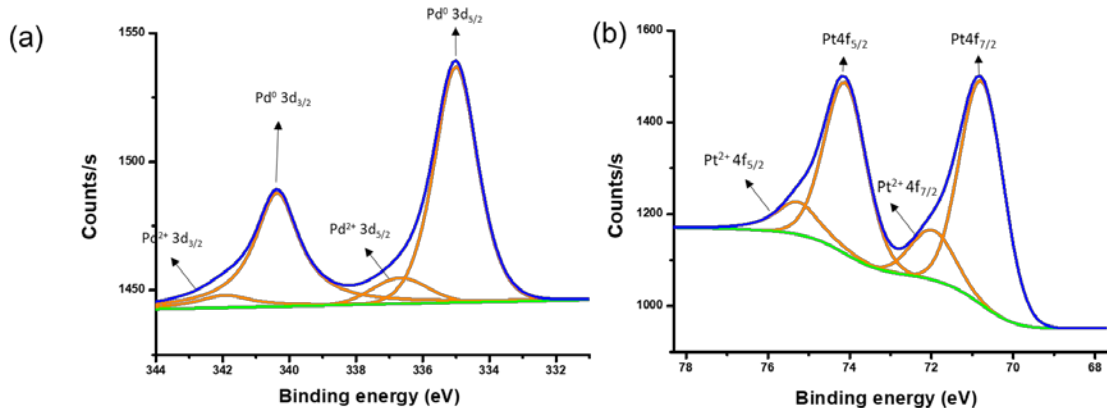


Fig. S18. The XPS data (a) Pd 4d peaks of Pd–Fe₃O₄ NPs after 15 cycle of the catalytic reactions (b) Pt 4f peaks of Pt–Fe₃O₄ NPs after 15 cycle of the catalytic reactions

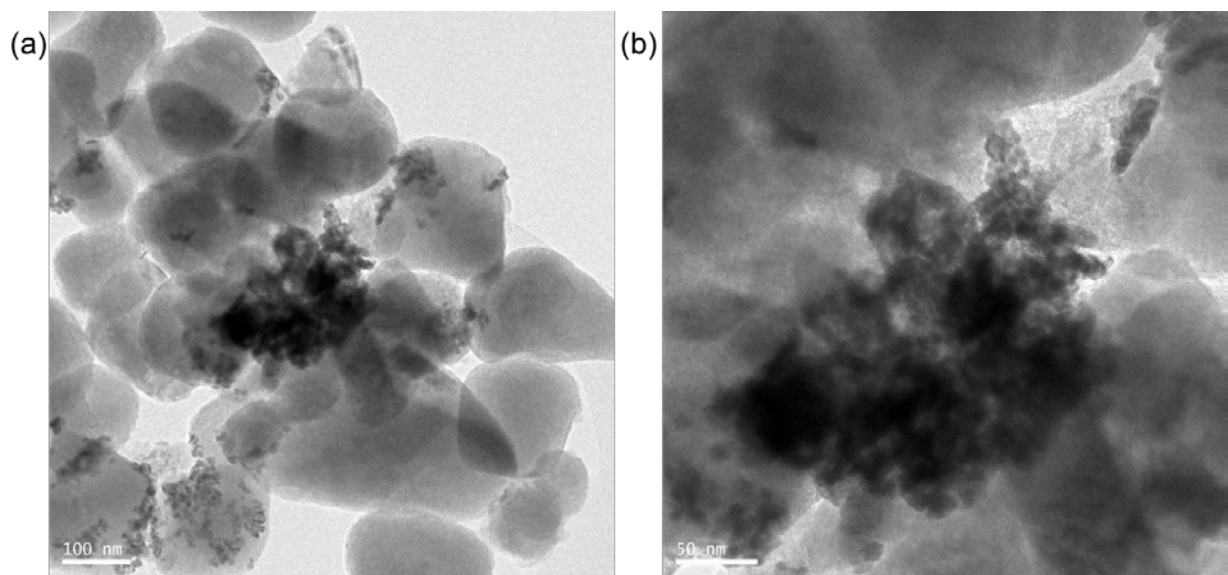


Fig. S19. (a) HR-TEM image of Spent Pd–Pt– Fe_3O_4 NPs (20 recycled); (b) expanded view.

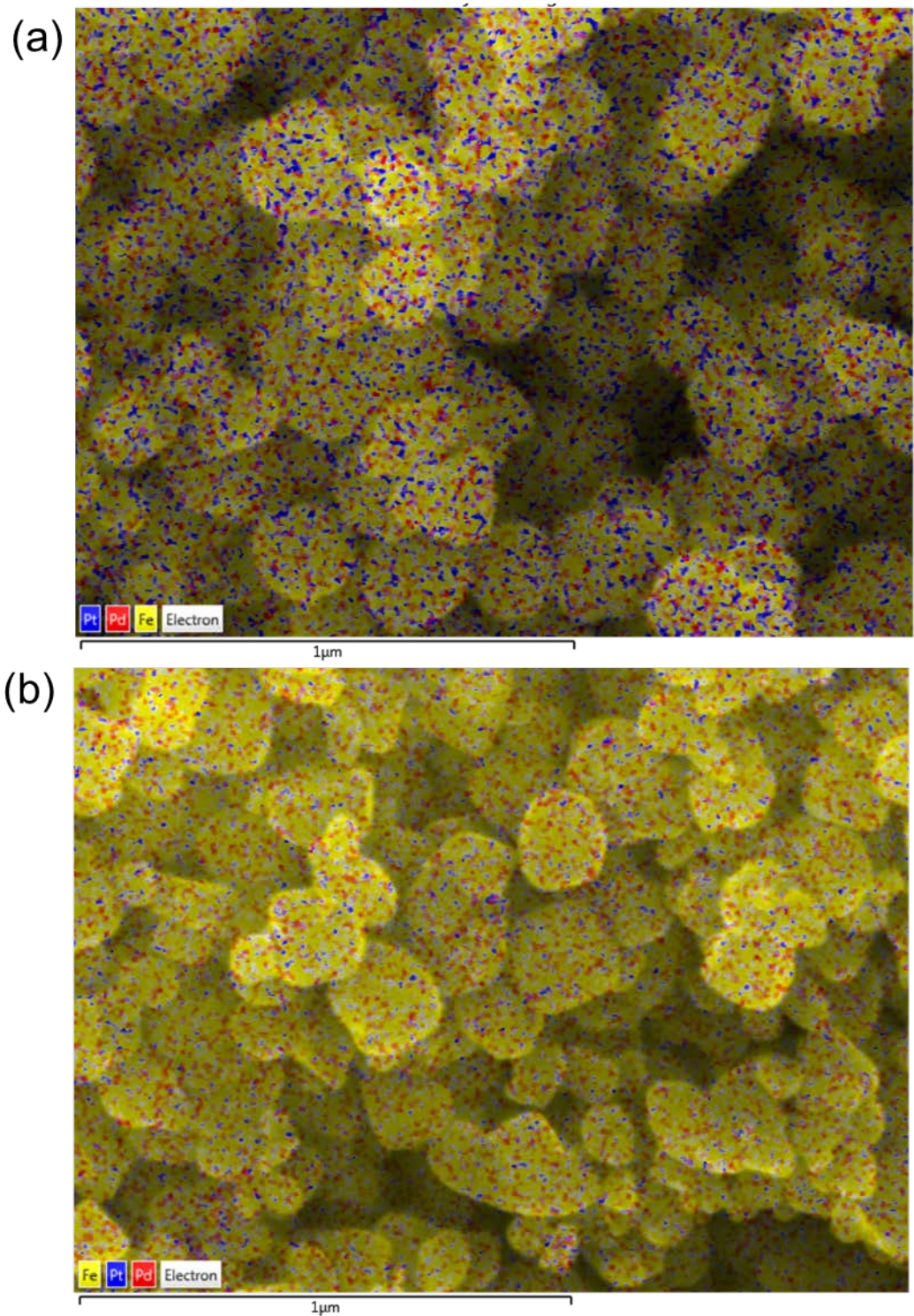


Fig. S20. The mapping images of (a) Fresh Pd–Pt– Fe_3O_4 NPs and (b) Spent Pd–Pt– Fe_3O_4 NPs (20 recycled).

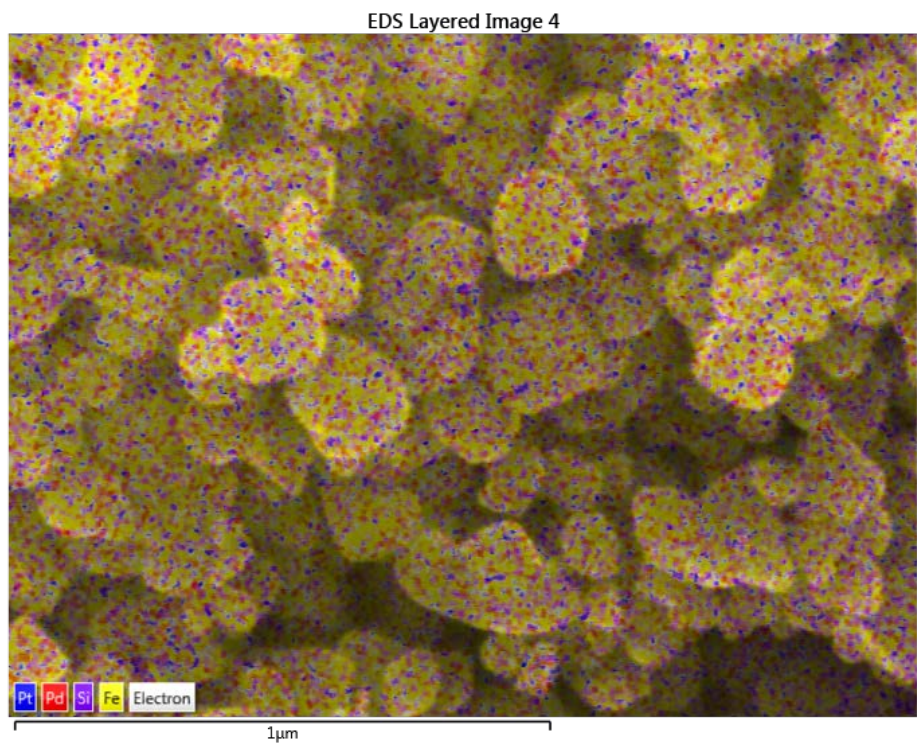


Fig. S21. SEM-EDS image of spent Pd–Pt–Fe₃O₄ NPs (20 recycled).

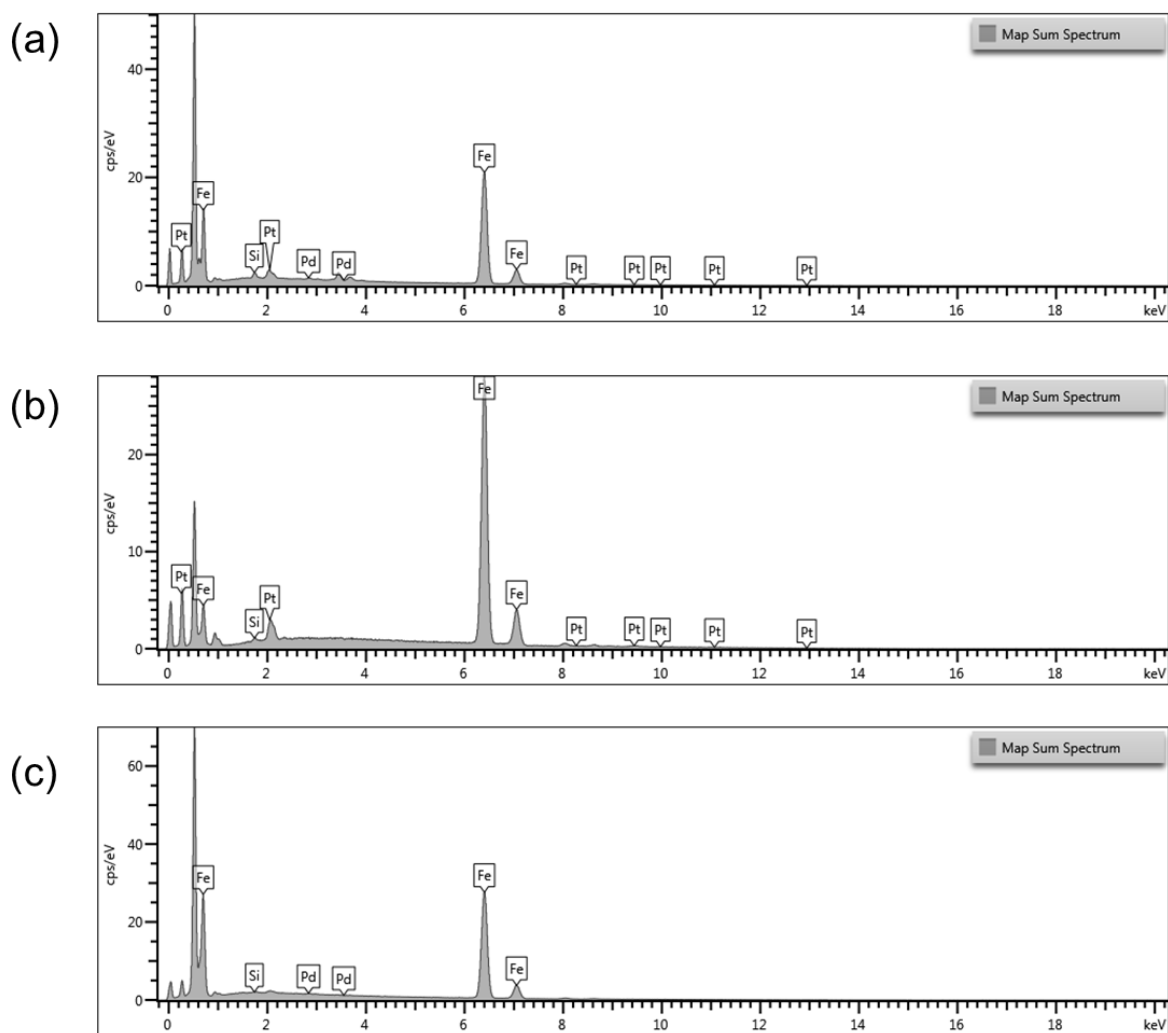


Fig. S22. SEM-EDS pattern: (a) spent Pd–Pt–Fe₃O₄ NPs (after 20 recycle); (b) spent Pt–Fe₃O₄ NPs (after 15 recycle); (c) spent Pd–Fe₃O₄ NPs (after 15 recycle).

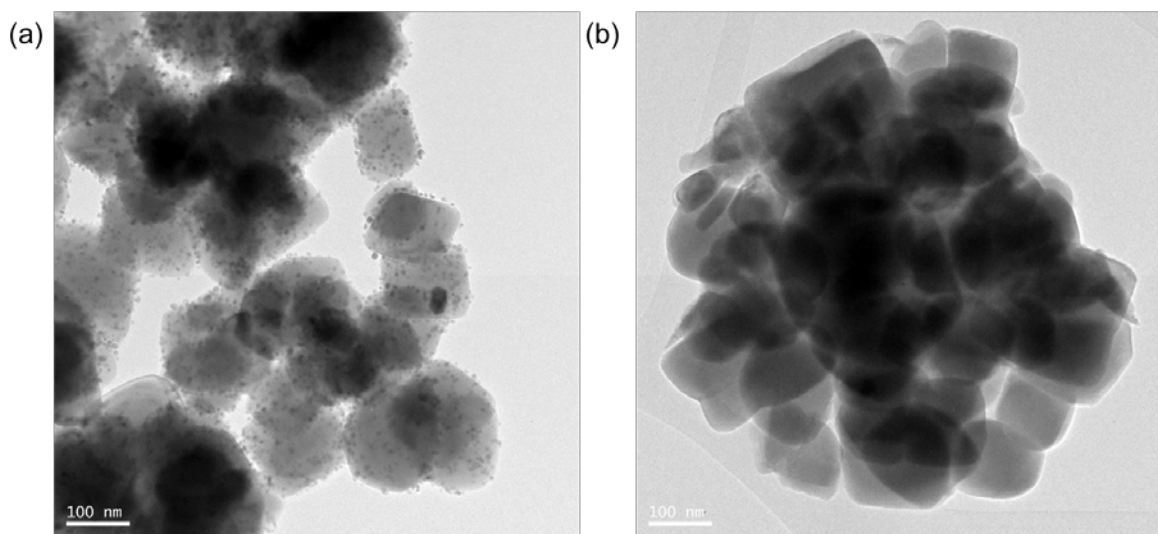


Fig. S23. (a) HR-TEM image of fresh $\text{Pd}-\text{Fe}_3\text{O}_4$ NPs and (b) HR-TEM image of spent $\text{Pd}-\text{Fe}_3\text{O}_4$ NPs (after 15 recycle).

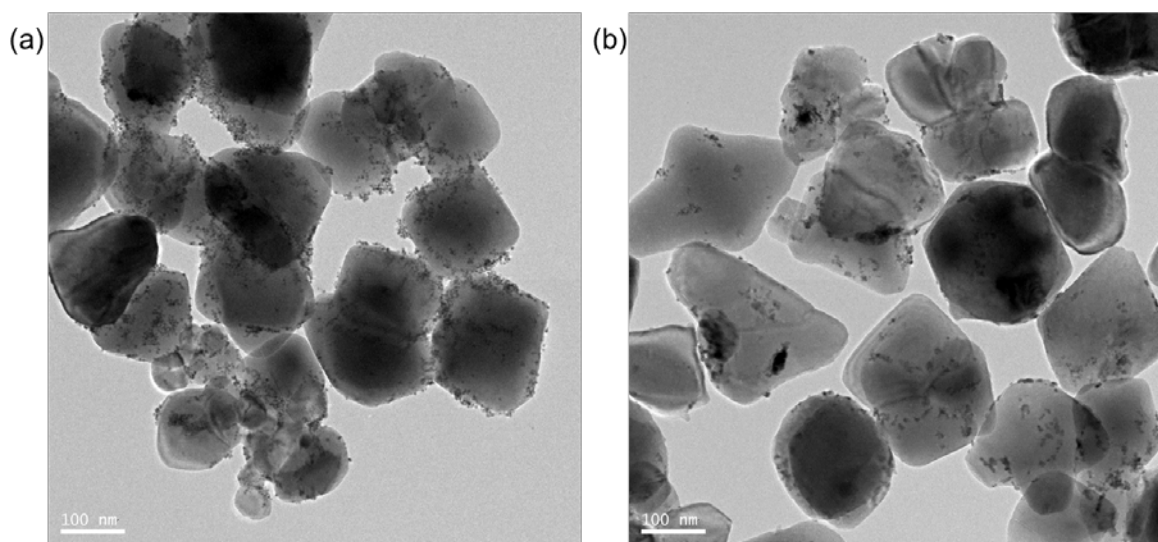
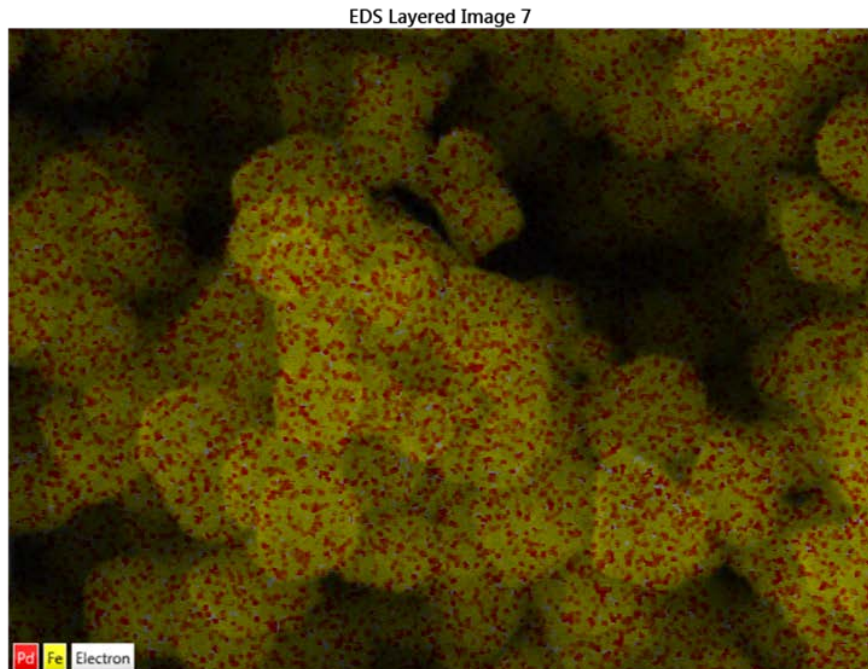


Fig. S24. (a) HR-TEM image of fresh $\text{Pt}-\text{Fe}_3\text{O}_4$ NPs and (b) HR-TEM image of Spent $\text{Pt}-\text{Fe}_3\text{O}_4$ NPs (after 15 recycle).

(a)



(b)

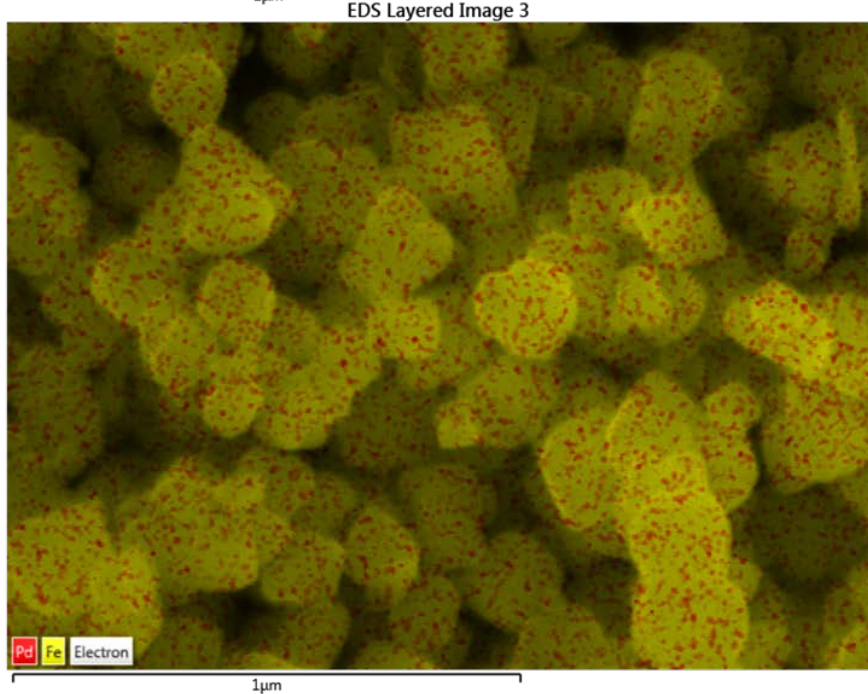
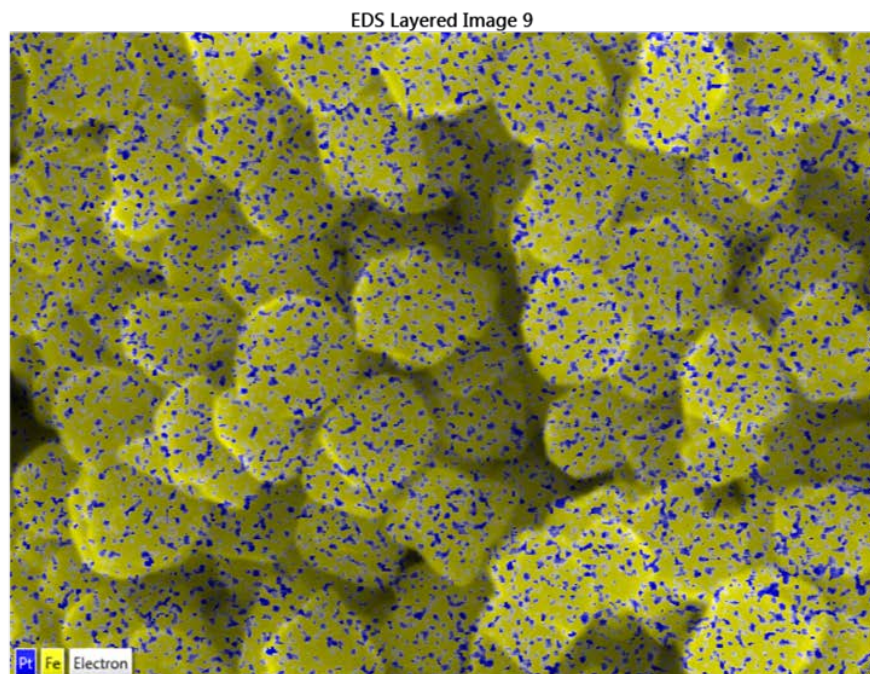


Fig. S25. The mapping images of (a) Fresh Pd– Fe_3O_4 NPs and (b) Spent Pd– Fe_3O_4 NPs (after 15 recycle)

(a)



(b)

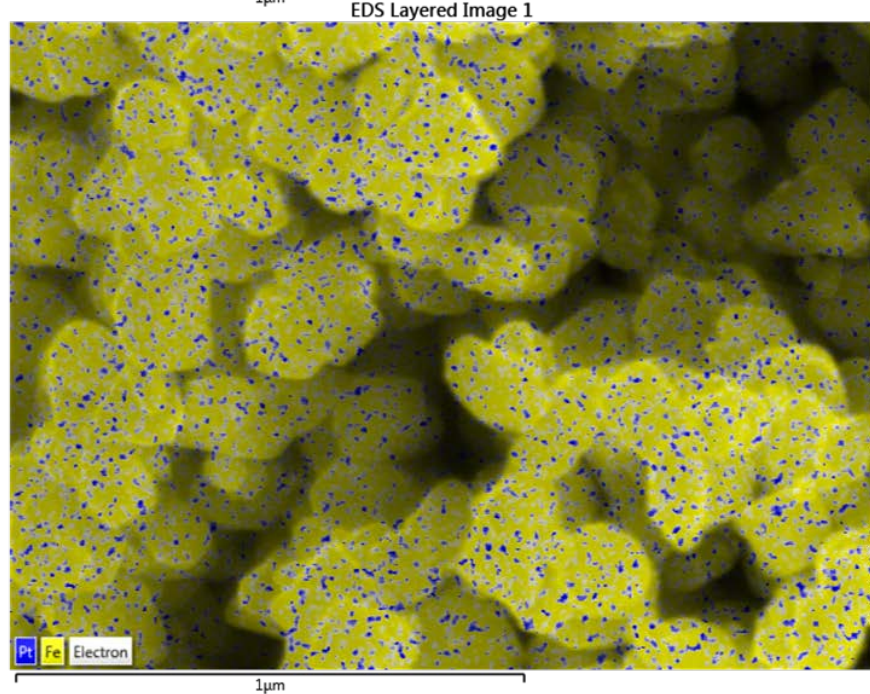


Fig. S26. The mapping images of (a) Fresh Pt–Fe₃O₄ NPs and (b) Spent Pt–Fe₃O₄ NPs (after 15 recycle).

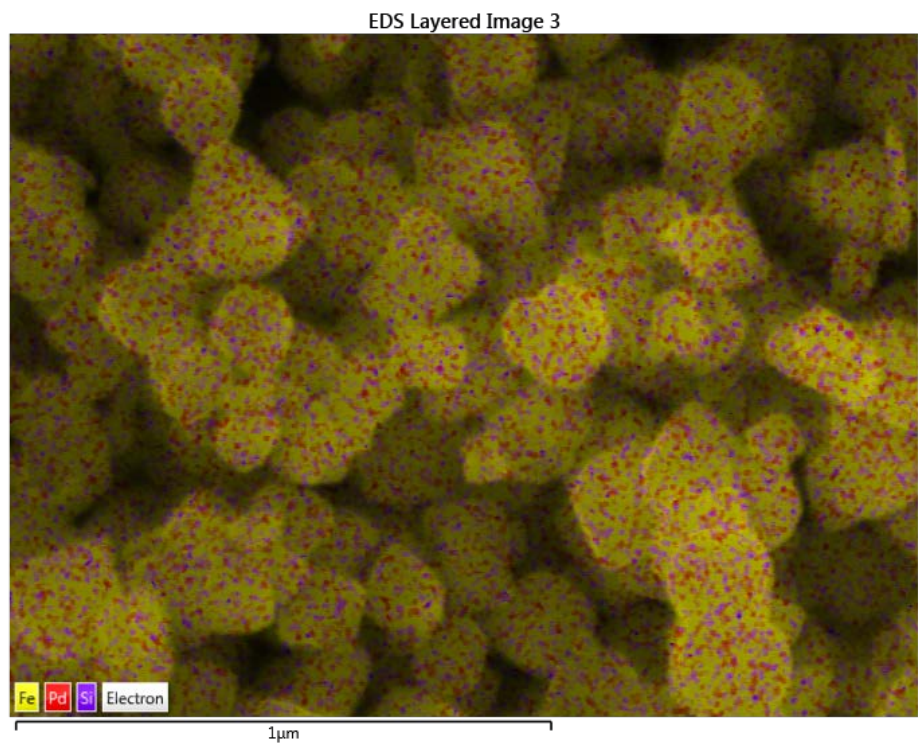


Fig. S27. SEM-EDS image of spent Pd–Fe₃O₄ NPs (after 15 recycle).

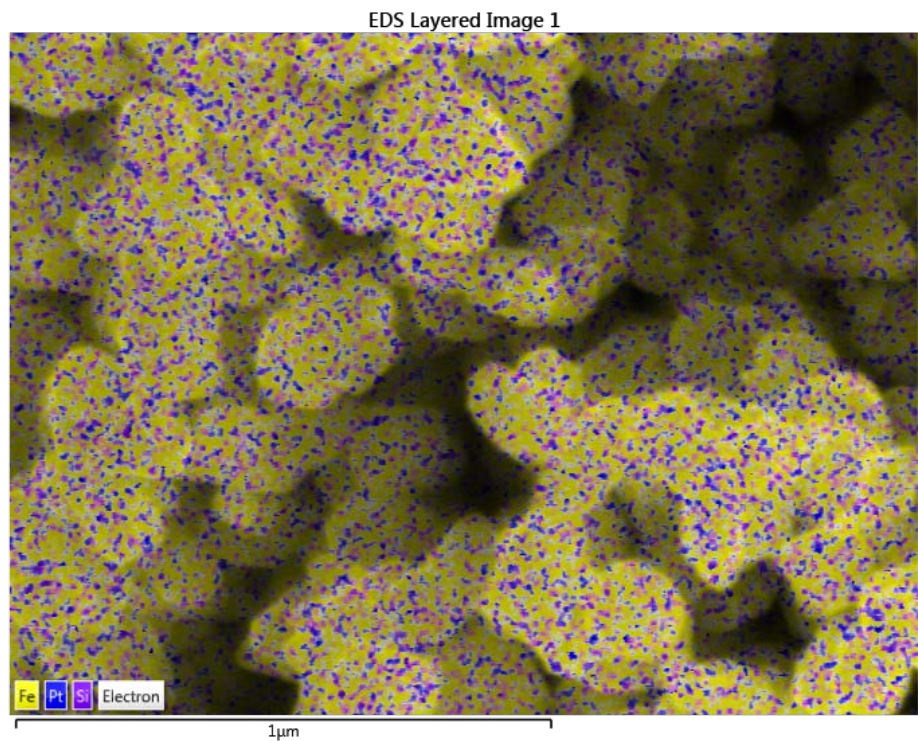


Fig. S28. SEM-EDS image of spent Pt–Fe₃O₄ NPs (after 15 recycle).

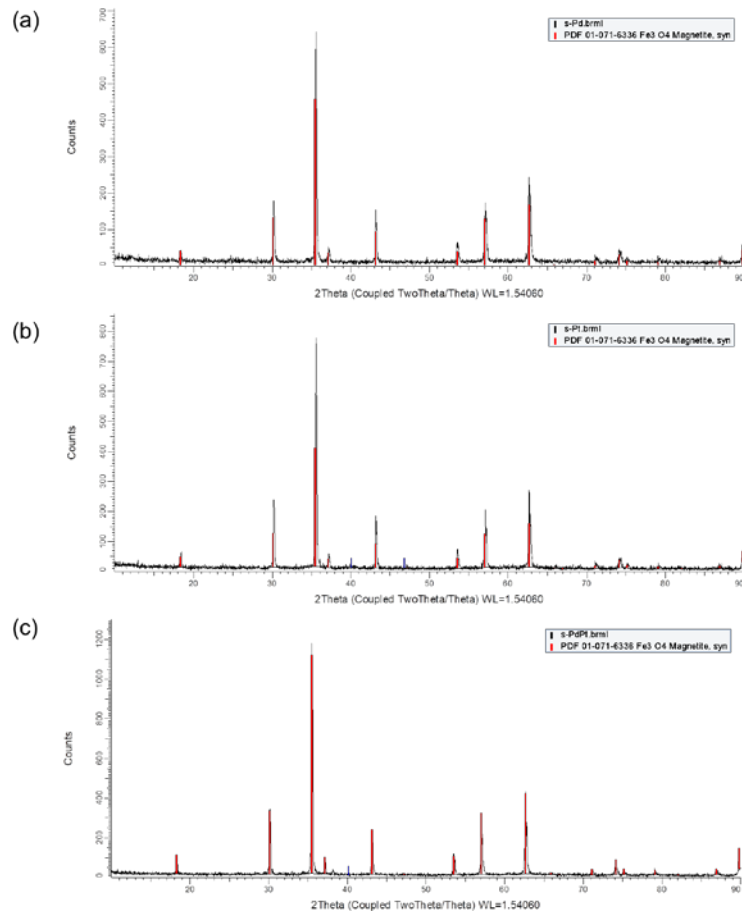


Fig. S29. The XRD data of (b) 15 cycle of Pd–Fe₃O₄ NPs; (c) 15 cycle of Pt–Fe₃O₄ NPs; (d) 20 cycle of Pd–Pt–Fe₃O₄ NPs

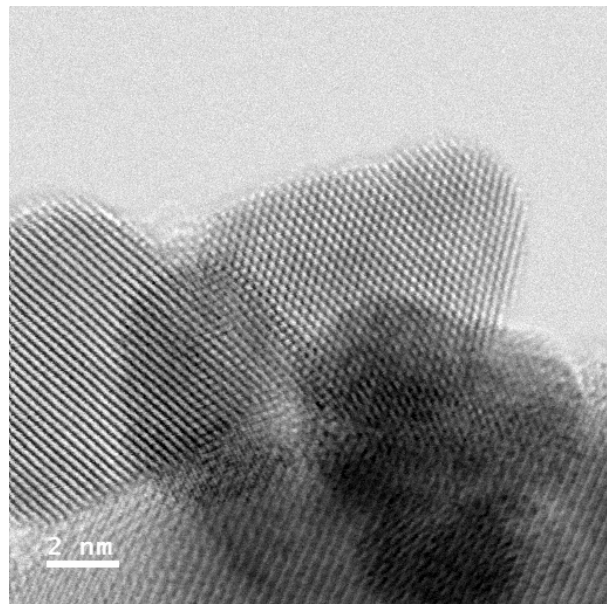


Fig. S30. BF-STEM image of Pd–Pt–Fe₃O₄ NPs

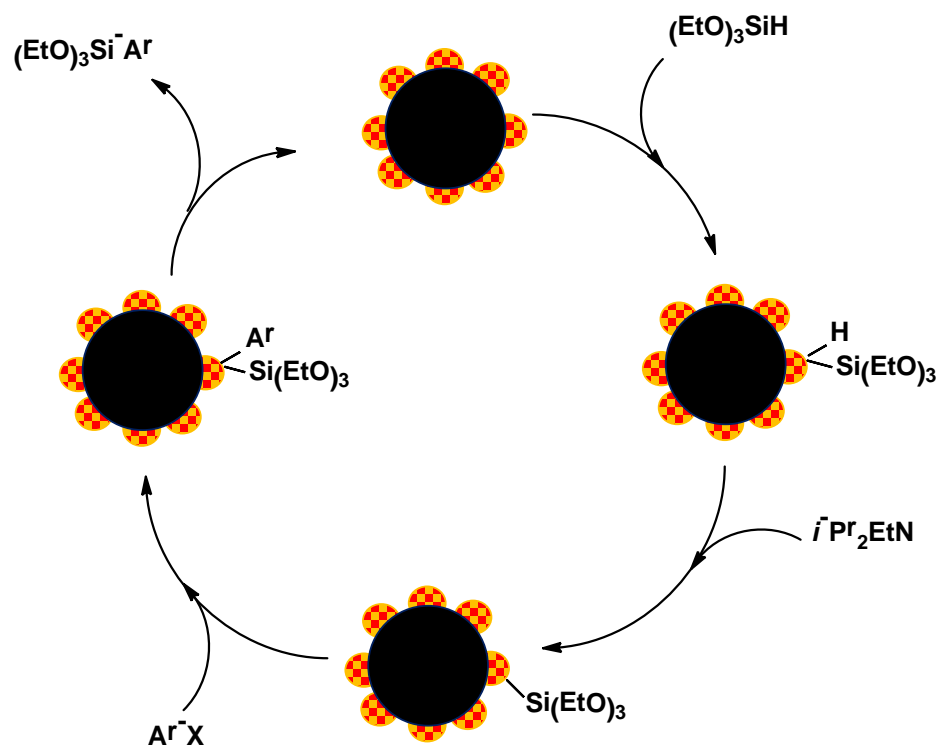
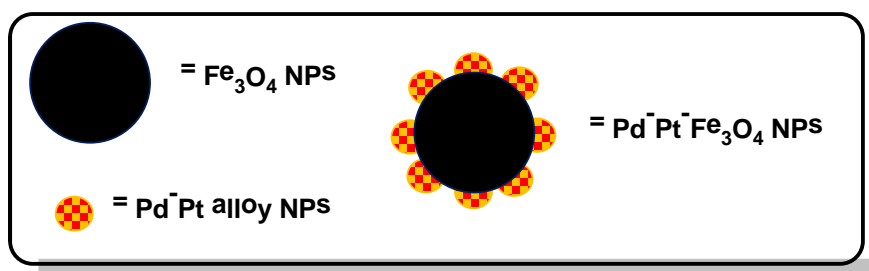


Fig. S31. Proposed reaction mechanism

Table S1. ICP data of fresh and spent Pd-Pt-Fe₃O₄ NPs

Sample	Pd (wt%)	Pt (wt%)
Fresh	4.10	9.60
After 20 reactions	3.35	6.83

Table S2. ICP data of fresh and spent Pd-Fe₃O₄ NPs

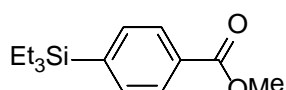
Sample	Pd (wt%)
Fresh	7.47
After 15 reactions	3.44

Table S3. ICP data of fresh and spent Pt-Fe₃O₄ NPs

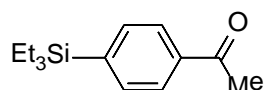
Sample	Pt (wt%)
Fresh	10.76
After 15 reactions	2.51

General Procedure for the Pd-Pt-Fe₃O₄ catalyzed arylsilylation.

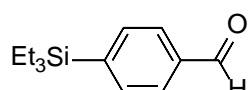
Aryl halide (0.7 mmol), diisopropylethylamine (136 mg, 1.05 mmol), Pd-Pt-Fe₃O₄ (70 mg, Pd 4.1 wt%, Pt 9.6 wt%, Pd base 3.77 mol%, Pt base 5 mol%), hydrosilane (1.05 mmol), and NMP (4 mL) were added to the reaction vial. The mixture was stirred at 70 °C for 15 h. After the mixture was extracted with Et₂O and water. The organic layer was dried over sodium sulfate. After then it was purified by chromatography on silica gel.



Methyl 4-(triethylsilyl)benzoate (2a)^[1] : Methyl 4-iodobenzene (183 mg, 0.7 mmol) and triethylsilane (122 mg, 1.05 mmol) afforded methyl 4-(triethylsilyl)benzoate (154 mg, 0.62 mmol, 88%) as a colorless oil; methyl 4-iodobenzene (150 mg, 0.7 mmol) and triethylsilane (122 mg, 1.05 mmol) afforded methyl 4-(triethylsilyl)benzoate (119 mg, 0.48 mmol, 68%) as a colorless oil; ¹H NMR (500 MHz, CDCl₃) δ 7.99 (m, 2H), 7.56 (m, 2H), 3.92 (s, 3H), 0.95 (m, 9H), 0.81 (m, 6H); ¹³C NMR (125 MHz, CDCl₃) δ 167.4, 144.1, 134.2, 130.2, 128.4, 52.1, 7.3, 3.2; MS (EI) m/z = 250 (M⁺).

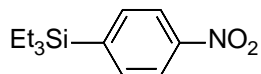


1-(4-(Triethylsilyl)phenyl)ethanone (2b)^[1] : 1-(4-Iodophenyl)ethanon (172 mg, 0.7 mmol) and triethylsilane (122 mg, 1.05 mmol) afforded 1-(4-(triethylsilyl)phenyl)ethanone (138 mg, 0.59 mmol, 84%) as a colorless oil; 1-(4-bromophenyl)ethanon (139 mg, 0.7 mmol) and triethylsilane (122 mg, 1.05 mmol) afforded 1-(4-(triethylsilyl)phenyl)ethanone (119 mg, 0.51 mmol, 73%) as a colorless oil; ¹H NMR (500 MHz, CDCl₃) δ 7.93 (m, 2H), 7.61 (m, 2H), 2.61 (s, 3H), 0.97 (m, 9H), 0.83 (m, 6H); ¹³C NMR (125 MHz, CDCl₃) δ 198.5, 144.5, 137.1, 134.4, 127.1, 26.6, 7.3, 3.2; MS (EI) m/z = 234 (M⁺).

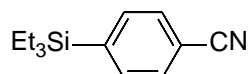


4-(Triethylsilyl)benzaldehyde (2c)^[1] : 4-Iodobenzaldehyde (162 mg, 0.7 mmol) and triethylsilane (122 mg, 1.05 mmol) afforded 4-(triethylsilyl)benzaldehyde (125 mg, 0.57 mmol, 81%) as a colorless oil; 4-bromobenzaldehyde (129 mg, 0.7 mmol) and triethylsilane (122 mg, 1.05 mmol) afforded 4-(triethylsilyl)benzaldehyde (94 mg, 0.43 mmol, 61%) as a

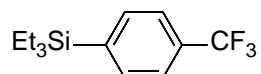
colorless oil; ^1H NMR (500 MHz, CDCl_3) δ 10.03 (s, 1H), 7.90 (d, $J = 8.2$ Hz, 2H), 7.67 (d, $J = 8.0$ Hz, 2H), 0.97 (m, 9H), 0.84 (m, 6H); ^{13}C NMR (125 MHz, CDCl_3) δ 192.5, 146.4, 136.2, 134.5, 128.3, 7.1, 2.9; MS (EI) m/z = 220 (M^+).



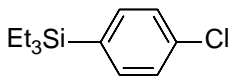
Triethyl(4-nitrophenyl)silane (2d)^[1] : 1-Iodo-4-nitrobenzene (174 mg, 0.7 mmol) and triethylsilane (122 mg, 1.05 mmol) afforded triethyl(4-nitrophenyl)silane (105 mg, 0.44 mmol, 63%) as a yellow oil; 1-bromo-4-nitrobenzene (94 mg, 0.7 mmol) and triethylsilane (122 mg, 1.05 mmol) afforded triethyl(4-nitrophenyl)silane (91 mg, 0.39 mmol, 55%) as a yellow oil; ^1H NMR (500 MHz, CDCl_3) δ 8.17 (d, $J = 8.6$ Hz, 2H), 7.66 (d, $J = 8.6$ Hz, 2H), 0.98-0.81 (m, 15H); ^{13}C NMR (125 MHz, CDCl_3) δ 148.4, 147.3, 135.0, 122.2, 7.2, 3.1; MS (EI) m/z = 237 (M^+).



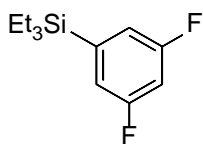
4-(Triethylsilyl)benzonitrile (2e)^[1] : 4-Iodobenzonitrile (160 mg, 0.7 mmol) and triethylsilane (122 mg, 1.05 mmol) afforded 4-(triethylsilyl)benzonitrile (112 mg, 0.52 mmol, 74%) as a colorless oil; 4-Iodobenzonitrile (126 mg, 0.7 mmol) and triethylsilane (122 mg, 1.05 mmol) afforded 4-(triethylsilyl)benzonitrile (96 mg, 0.39 mmol, 63%) as a colorless oil; ^1H NMR (500 MHz, CDCl_3) δ 7.60 (m, 4H), 0.96 (m, 9H), 0.82 (m, 6H); ^{13}C NMR (125 MHz, CDCl_3) δ 144.9, 134.8, 131.1, 119.3, 112.5, 7.5, 3.3; MS (EI) m/z = 217 (M^+).



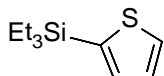
Triethyl(4-(trifluoromethyl)phenyl)silane (2f)^[1] : 1-Iodo-4-(trifluoromethyl)benzene (190 mg, 0.7 mmol) and triethylsilane (122 mg, 1.05 mmol) afforded triethyl(4-(trifluoromethyl)phenyl)silane (82 mg, 0.32 mmol, 45%) as a colorless oil; 1-bromo-4-(trifluoromethyl)benzene (157 mg, 0.7 mmol) and triethylsilane (122 mg, 1.05 mmol) afforded triethyl(4-(trifluoromethyl)phenyl)silane (36 mg, 0.14 mmol, 20%) as a colorless oil; ^1H NMR (500 MHz, CDCl_3) δ 7.60 (q, $J = 8.4$ Hz, 4H), 0.97 (m, 9H), 0.82 (m, 6H); ^{13}C NMR (125 MHz, CDCl_3) δ 142.6, 134.4, 130.6 ($J_{\text{C}-\text{F}} = 31.9$ Hz), 124.3 ($J_{\text{C}-\text{F}} = 270.6$ Hz), 124.1 ($J_{\text{C}-\text{F}} = 3.8$ Hz), 7.3, 3.2; MS (EI) m/z = 260 (M^+).



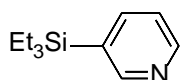
(4-Chlorophenyl)triethylsilane (2g): 1-Chloro-4-iodobenzene (167 mg, 0.7 mmol) and triethylsilane (122 mg, 1.05 mmol) afforded (4-chlorophenyl)triethylsilane (133 mg, 0.59 mmol, 84%) as a colorless oil; 1-bromo-4-chlorobenzene (133 mg, 0.7 mmol) and triethylsilane (122 mg, 1.05 mmol) afforded (4-chlorophenyl)triethylsilane (116 mg, 0.51 mmol, 73%) as a colorless oil; ^1H NMR (500 MHz, CDCl_3) δ 7.41 (dt, $J = 8.4$ Hz, 1.9 Hz, 2H), 7.32 (dt, $J = 8.4$ Hz, 1.8 Hz, 2H), 0.95 (m, 9H), 0.77 (m, 6H); ^{13}C NMR (125 MHz, CDCl_3) δ 135.7, 135.5, 135.0, 127.9, 7.3, 3.3; MS (EI) m/z = 226 (M^+).



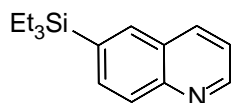
(3,5-difluorophenyl)triethylsilane (2h): 1,3-Difluoro-5-iodobenzene (167 mg, 0.7 mmol) and triethylsilane (122 mg, 1.05 mmol) afforded (3,5-difluorophenyl)triethylsilane (141 mg, 0.62 mmol, 88%) as a colorless oil; 1,3-Difluoro-5-iodobenzene (134 mg, 0.7 mmol) and triethylsilane (122 mg, 1.05 mmol) afforded (3,5-difluorophenyl)triethylsilane (109 mg, 0.48 mmol, 68%) as a colorless oil; ^1H NMR (500 MHz, CDCl_3) δ 6.96 (dt, $J = 6.0$ Hz, 2.3 Hz, 2H), 6.76 (tt, $J = 9.2$ Hz, 2.4 Hz, 1H), 0.95 (m, 9H), 0.78 (m, 6H); ^{13}C NMR (125 MHz, CDCl_3) δ 162.8 ($J_{\text{C}-\text{F}} = 250.0$ Hz, 10.5 Hz), 142.6 ($J_{\text{C}-\text{F}} = 9.4$ Hz), 116.0 ($J_{\text{C}-\text{F}} = 16.7$ Hz, 4.5 Hz), 104.0 ($J_{\text{C}-\text{F}} = 24.9$ Hz), 7.2, 3.1; HRMS (EI) calcd. for $\text{C}_{12}\text{H}_{18}\text{F}_2\text{Si}$ [M]⁺ 228.1146 found 228.1146.



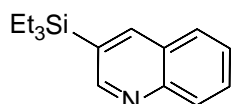
2-(Triethylsilyl)thiophene (2i): 2-Iodothiophene (92 mg, 0.7 mmol) and triethylsilane (122 mg, 1.05 mmol) afforded 2-(triethylsilyl)thiophene (110 mg, 0.56 mmol, 79%) as a colorless oil; 2-bromothiophene (113 mg, 0.7 mmol) and triethylsilane (122 mg, 1.05 mmol) afforded 2-(triethylsilyl)thiophene (76 mg, 0.39 mmol, 55%) as a colorless oil; ^1H NMR (500 MHz, CDCl_3) δ 7.61 (dd, $J = 4.6$ Hz, 0.9 Hz, 1H), 7.26 (dd, $J = 3.3$ Hz, 0.9 Hz, 1H), 7.21 (dd, $J = 4.6$ Hz, 3.3 Hz, 1H), 1.00 (m, 9H), 0.81 (m, 6H); ^{13}C NMR (125 MHz, CDCl_3) δ 136.5, 134.6, 130.4, 128.0, 7.4, 4.5; MS (EI) m/z = 198 (M^+).



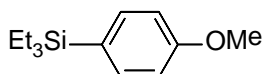
3-(Triethylsilyl)pyridine (2j)^[1] : 3-Iodopyridine (143 mg, 0.7 mmol) and triethylsilane (122 mg, 1.05 mmol) afforded 3-(triethylsilyl)pyridine (104 mg, 0.54 mmol, 77%) as a colorless oil; 3-bromopyridine (110 mg, 0.7 mmol) and triethylsilane (122 mg, 1.05 mmol) afforded 3-(Triethylsilyl)pyridine (83 mg, 0.43 mmol, 61%) as a colorless oil; ¹H NMR (500 MHz, CDCl₃) δ 8.67 (s, 1H), 8.58 (d, *J* = 3.6 Hz, 1H), 7.77 (dt, *J* = 7.5 Hz, 1.9 Hz, 1H), 7.26 (ddd, *J* = 7.5 Hz, 4.9 Hz, 0.9 Hz, 1H), 0.98 (m, 9H), 0.82 (m, 6H); ¹³C NMR (125 MHz, CDCl₃) δ 154.4, 149.7, 142.0, 132.3, 123.2, 7.2, 3.0; MS (EI) m/z = 193 (M⁺).



6-(Triethylsilyl)quinoline (2k)^[3] : 3-iodoquinoline (178 mg, 0.7 mmol) and triethylsilane (122 mg, 1.05 mmol) afforded 6-(triethylsilyl)quinoline (138 mg, 0.57 mmol, 81%) as a colorless oil; 3-bromoquinoline (113 mg, 0.7 mmol) and triethylsilane (122 mg, 1.05 mmol) afforded 6-(triethylsilyl)quinoline (131 mg, 0.54 mmol, 77%) as a colorless oil; ¹H NMR (500 MHz, CDCl₃) δ 8.93 (bs, 1H), 8.19 (d, *J* = 8.4 Hz, 1H), 8.11 (d, *J* = 8.4 Hz, 1H), 7.96 (s, 1H), 7.84 (dd, *J* = 8.4 Hz, 1.4 Hz, 1H), 7.43 (dd, *J* = 8.3 Hz, 4.25 Hz, 1H), 1.01 (m, 9H), 0.90 (m, 6H); ¹³C NMR (125 MHz, CDCl₃) δ 150.2, 148.1, 136.4, 136.2, 134.4, 134.3, 127.8, 127.6, 120.8, 7.2, 3.1; MS (EI) m/z = 243 (M⁺).

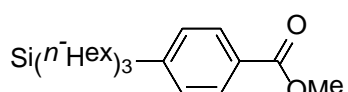


3-(Triethylsilyl)quinoline (2l)^[3] : 3-bromoquinoline (113 mg, 0.7 mmol) and triethylsilane (122 mg, 1.05 mmol) afforded 3-(triethylsilyl)quinoline (54 mg, 0.28 mmol, 39%) as a colorless oil; ¹H NMR (500 MHz, CDCl₃) δ 8.92 (bs, 1H), 8.18 (d, *J* = 7.4 Hz, 1H), 8.10 (d, *J* = 8.4 Hz, 1H), 7.96 (s, 1H), 7.83 (dd, *J* = 8.4 Hz, 1.4 Hz, 1H), 7.42 (dd, *J* = 8.3 Hz, 4.3 Hz, 1H), 1.00 (m, 9H), 0.89 (m, 6H); ¹³C NMR (125 MHz, CDCl₃) δ 150.4, 148.3, 136.6, 136.4, 134.6, 134.5, 128.0, 127.8, 121.0, 7.4, 3.3; MS (EI) m/z = 243 (M⁺).



Triethyl(4-methoxyphenyl)silane (2n)^[5] : 4-Iodoanisole (164 mg, 0.7 mmol) and triethylsilane (122 mg, 1.05 mmol) afforded triethyl(4-

methoxyphenyl)silane (29 mg, 0.13 mmol, 18%) as a colorless oil; 4-bromoanisole (131 mg, 0.7 mmol) afforded triethyl(4-methoxyphenyl)silane (11 mg, 0.05 mmol, 7%) as a colorless oil; ^1H NMR (500 MHz, CDCl_3) δ 7.43 (d, J = 8.7 Hz, 2H), 6.92 (d, J = 8.6 Hz, 2H), 3.83 (s, 3H), 0.97 (m, 9H), 0.78 (m, 6H); ^{13}C NMR (125 MHz, CDCl_3) δ 160.1, 135.5, 128.1, 113.4, 55.0, 7.4, 3.5; MS (EI) m/z = 222 (M^+).

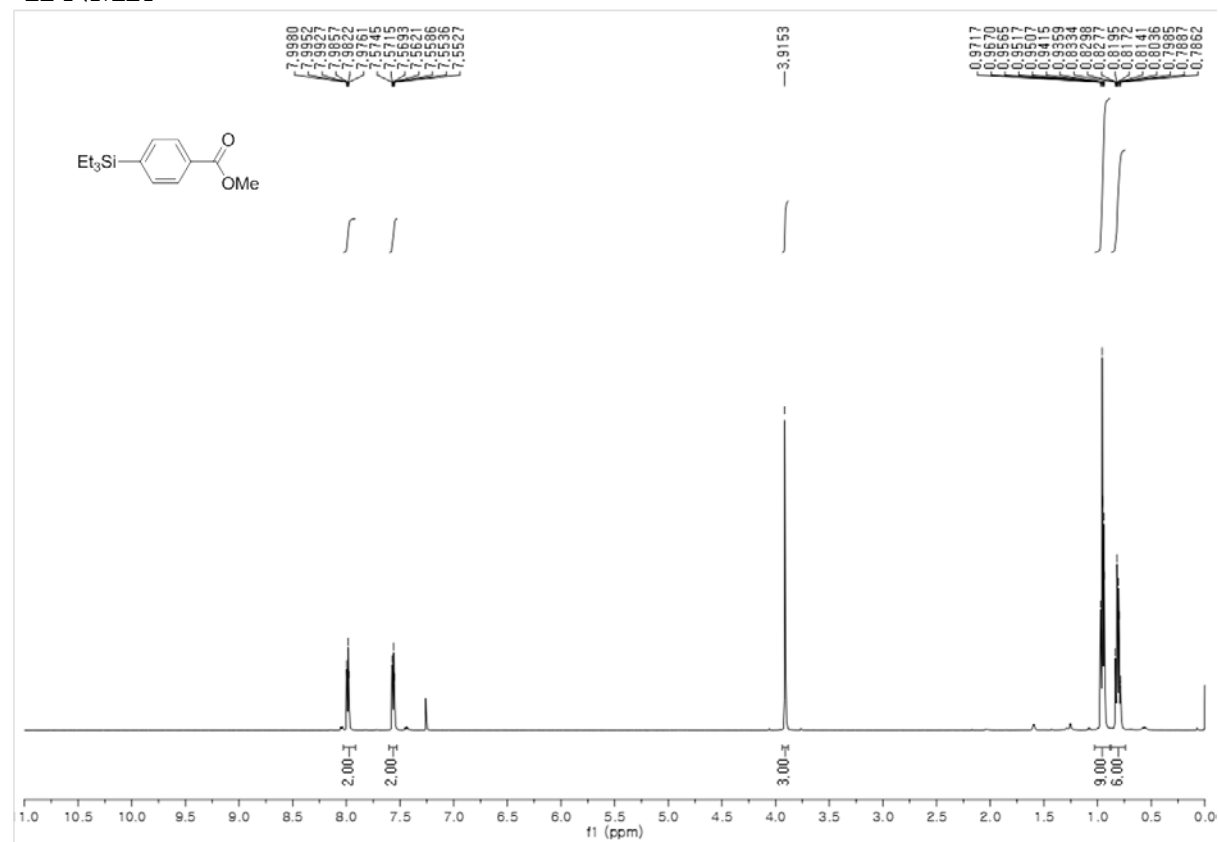


(3,5-difluorophenyl)triethylsilane (2h): Methyl 4-iodobenzene (183 mg, 0.7 mmol) and trihexylsilane (286 mg, 1.05 mmol) afforded methyl 4-(triethylsilyl)benzoate (246 mg, 0.59 mmol, 84%) as a colorless oil; methyl 4-iodobenzene (150 mg, 0.7 mmol) and trihexylsilane (286 mg, 1.05 mmol) afforded methyl 4-(triethylsilyl)benzoate (184 mg, 0.44 mmol, 63%) as a colorless oil; ^1H NMR (500 MHz, CDCl_3) δ 6.96 (dt, J = 6.0 Hz, 2.3 Hz, 2H), 6.76 (tt, J = 9.2 Hz, 2.4 Hz, 1H), 0.95 (m, 9H), 0.78 (m, 6H); ^{13}C NMR (125 MHz, CDCl_3) δ 162.8 ($J_{\text{C-F}}$ = 250.0 Hz, 10.5 Hz), 142.6 ($J_{\text{C-F}}$ = 9.4 Hz), 116.0 ($J_{\text{C-F}}$ = 16.7 Hz, 4.5 Hz), 104.0 ($J_{\text{C-F}}$ = 24.9 Hz), 7.2, 3.1; HRMS (EI) calcd. for $\text{C}_{12}\text{H}_{18}\text{F}_2\text{Si}$ [M] $^+$ 228.1146 found 228.1146.

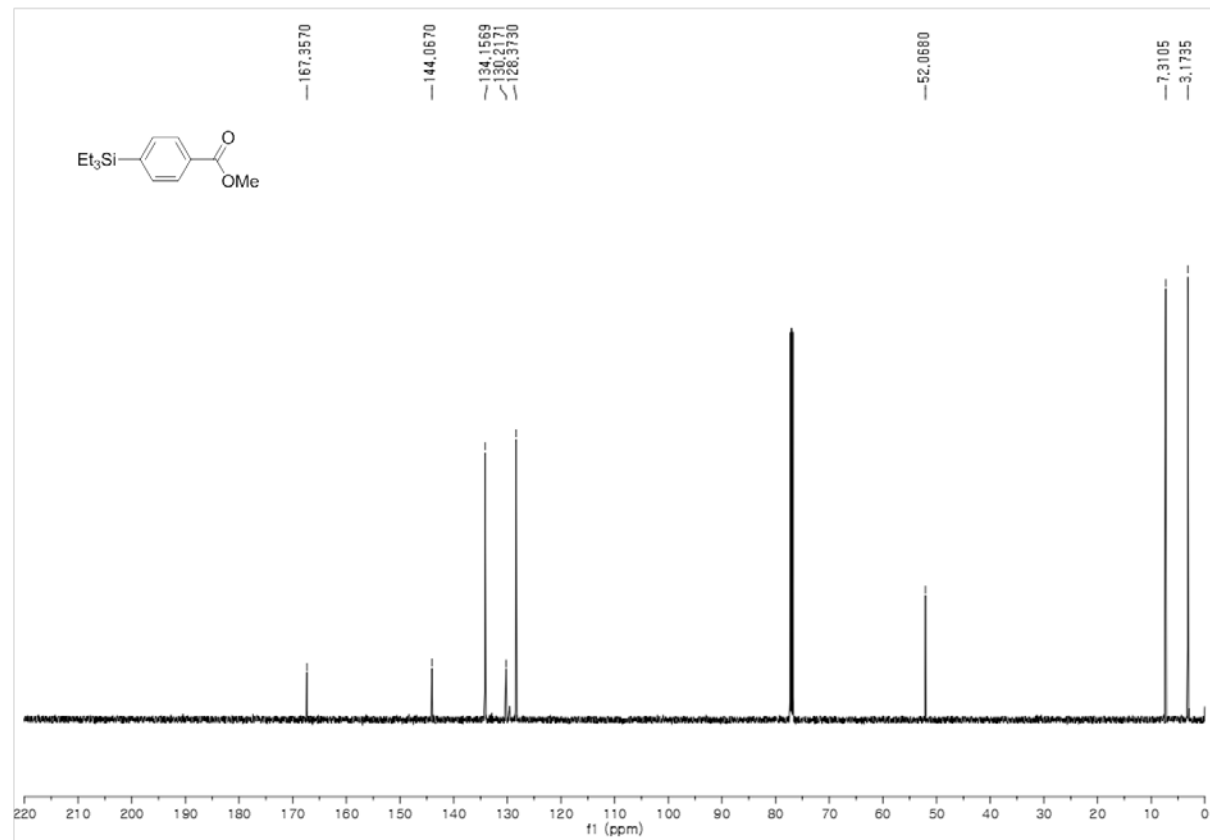
References

- [1] A. Hamze, O. Provot, M. Alami, J.-D. Brion, *Org. Lett.* **2006**, 8, 931.
- [2] N. Iranpoor, H. Firouzabadi, R. Azadi, *J. Organomet. Chem.* **2010**, 695, 887.
- [3] E. Lukevices, I. Segals, T. Lapina, *Vestis. Lat. Psr. Zinat. Akad.* **1978**, 3, 371.
- [4] K.-S. Lee, D. Katsoulis, J. Choi, *ACS Catal.* **2016**, 6, 1493.
- [5] Y. Yamanoi, H. Nishihara, *J. Org. Chem.* **2008**, 73, 6671.

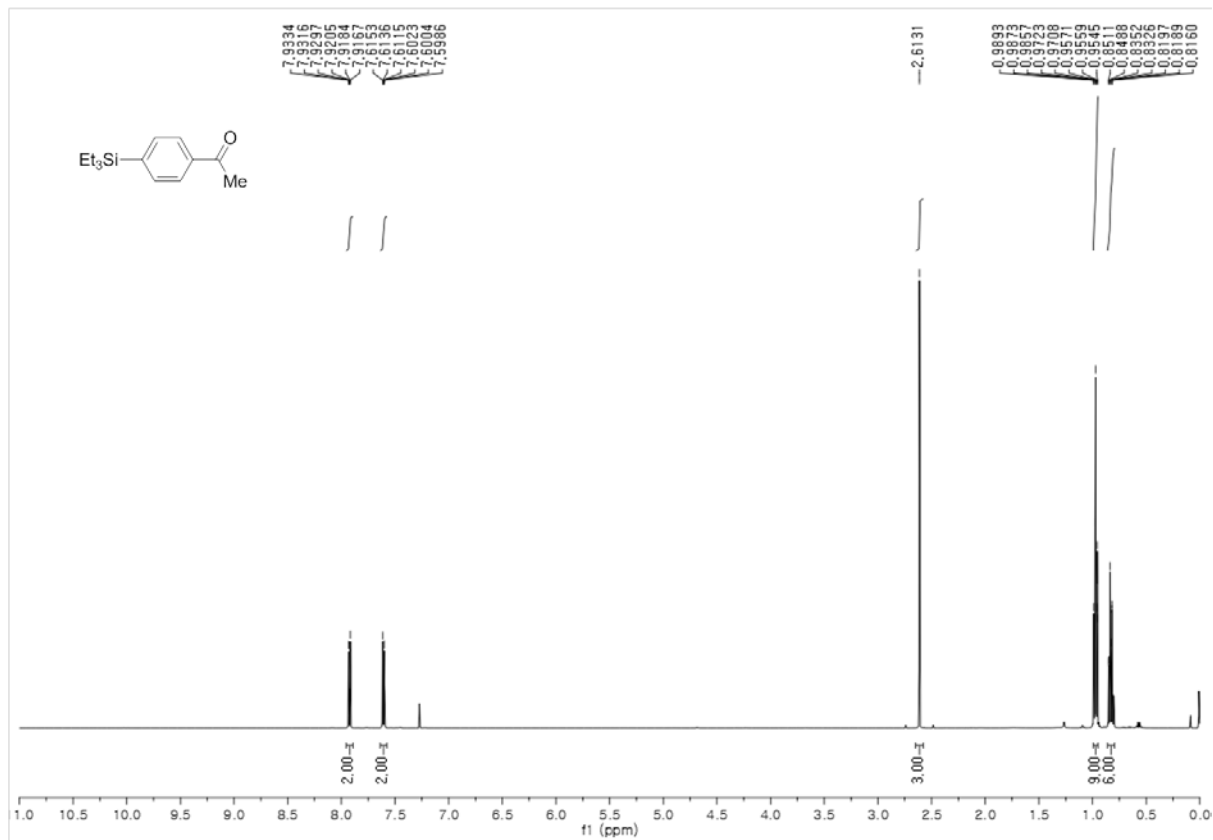
Methyl 4-(triethylsilyl)benzoate (2a)
 ^1H NMR



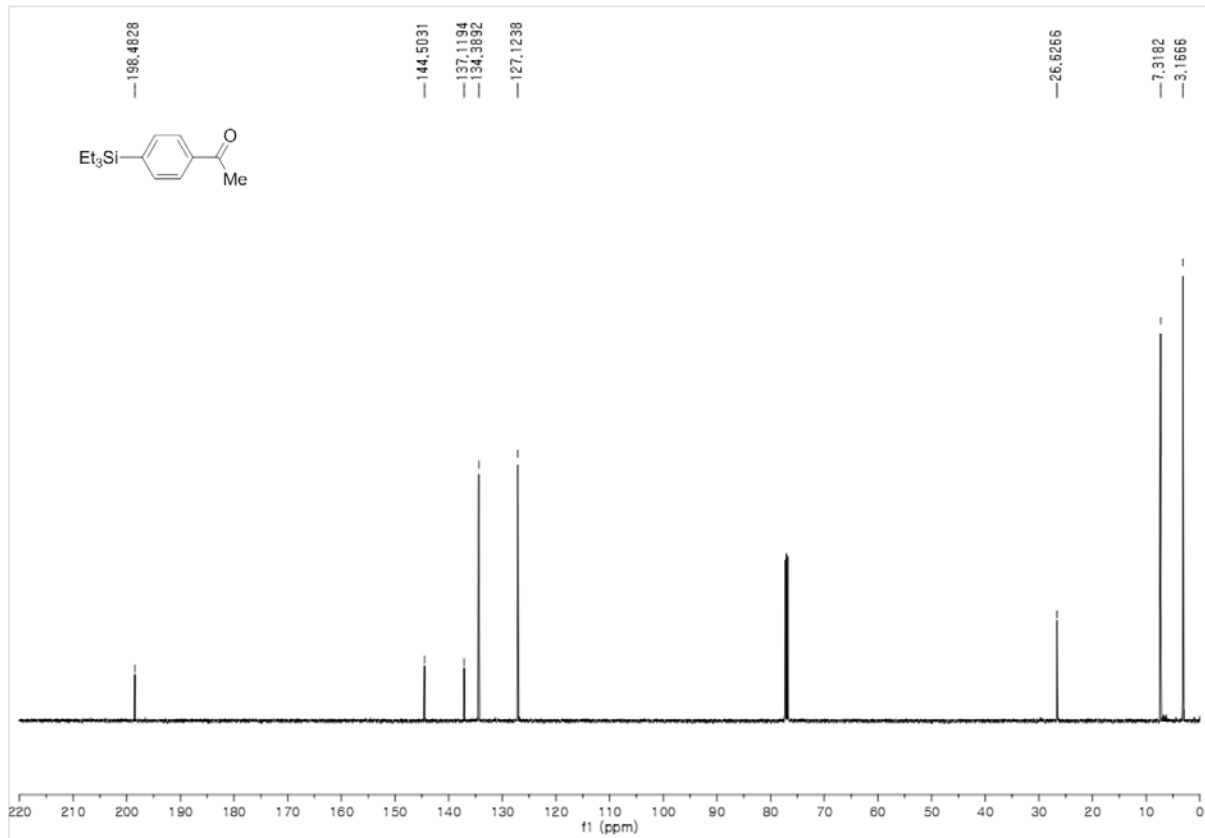
^{13}C NMR



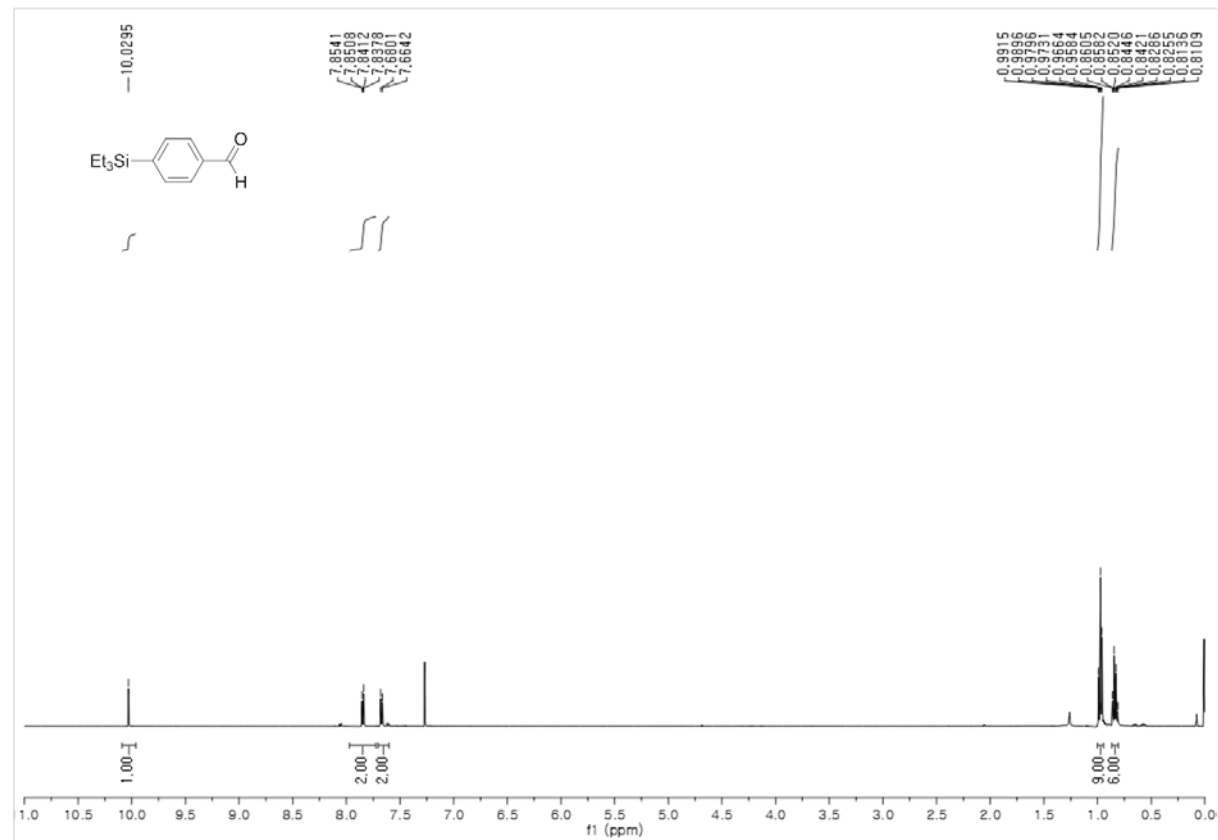
1-(4-(Triethylsilyl)phenyl)ethanone (2b)
 ^1H NMR



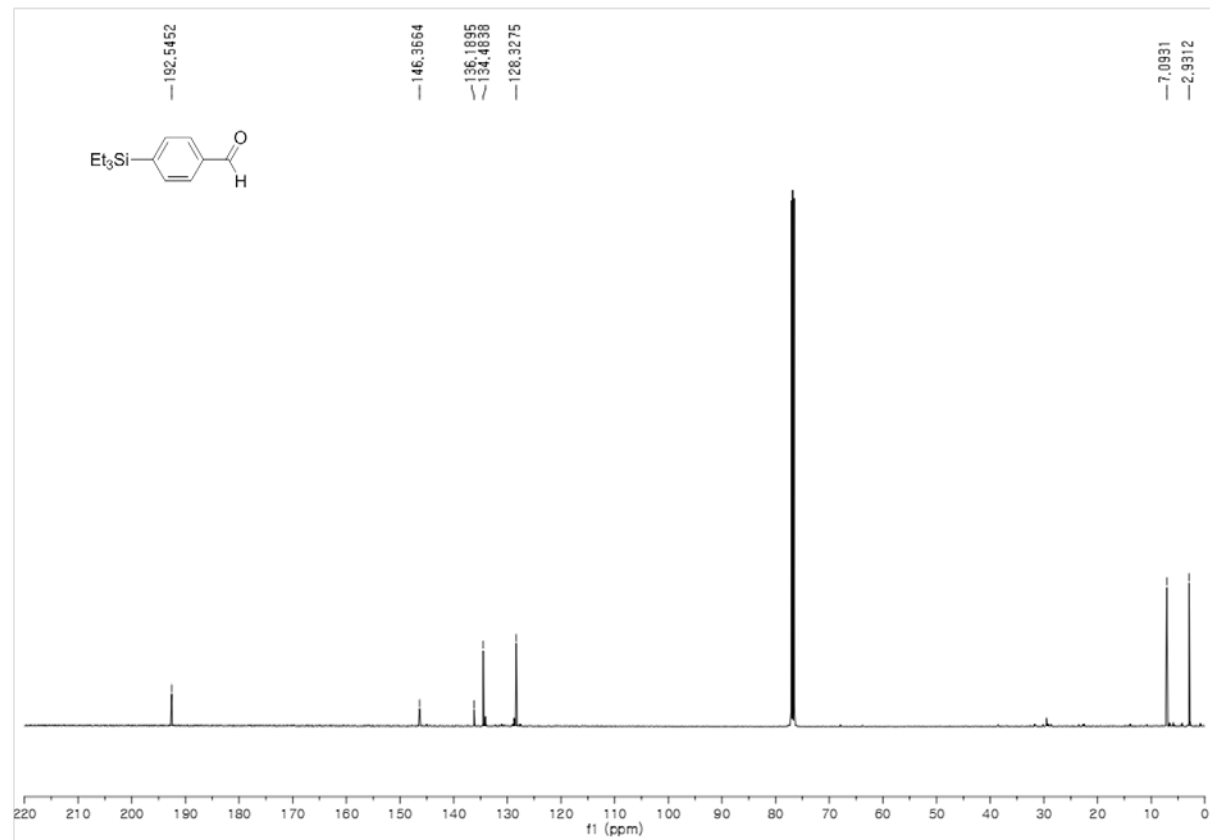
^{13}C NMR



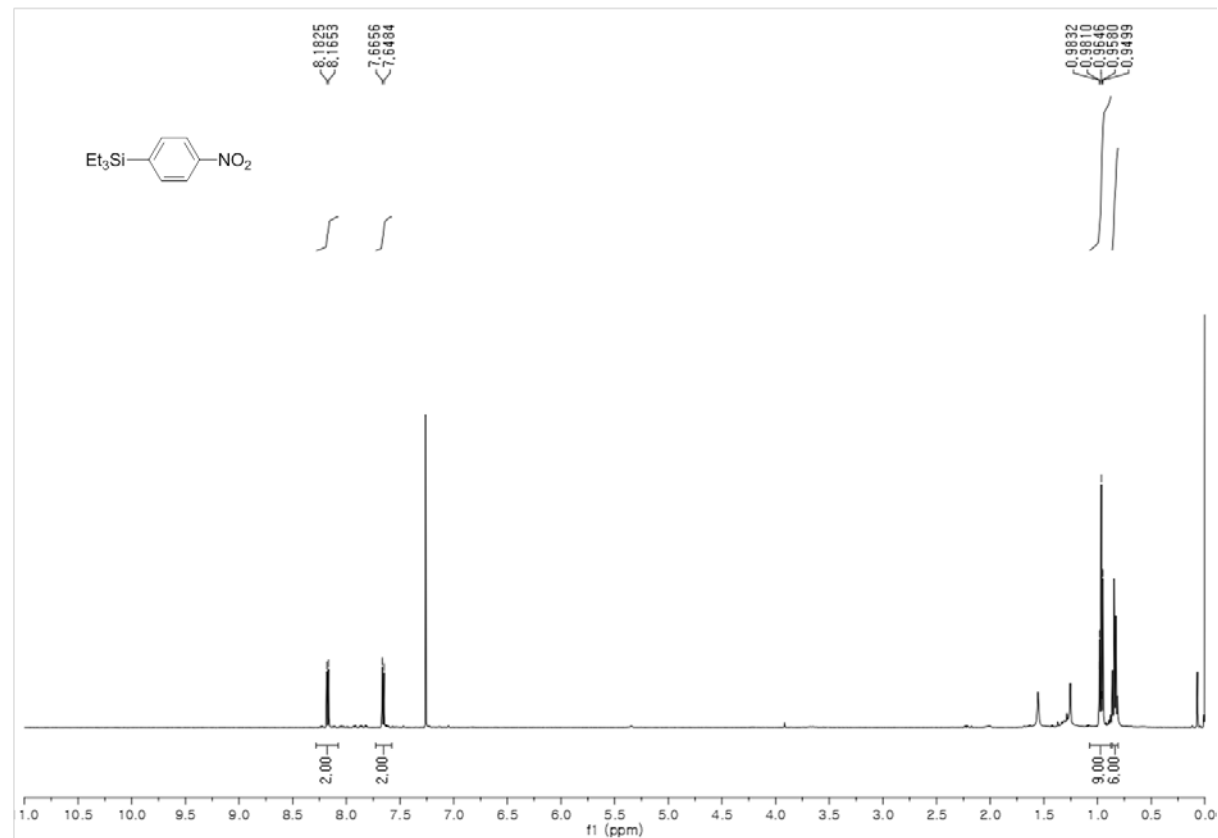
4-(Triethylsilyl)benzaldehyde (2c)
 ^1H NMR



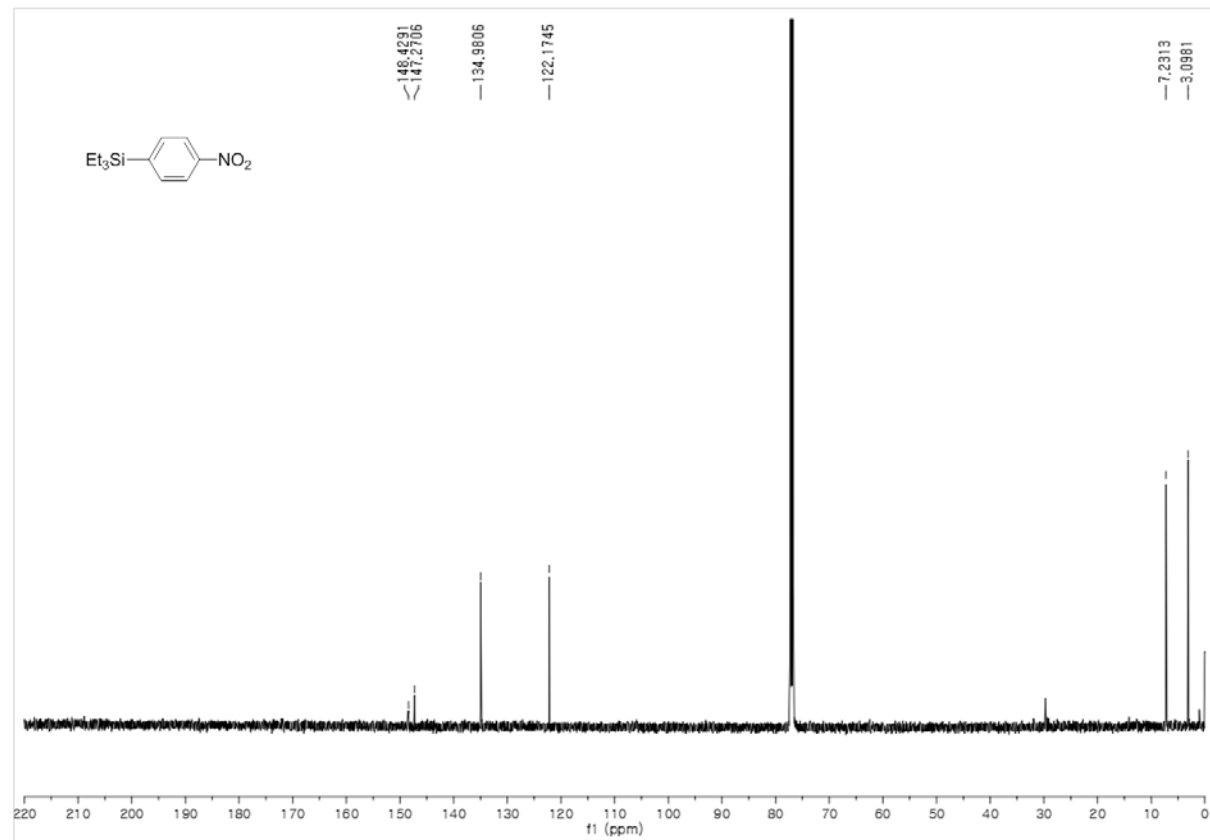
^{13}C NMR



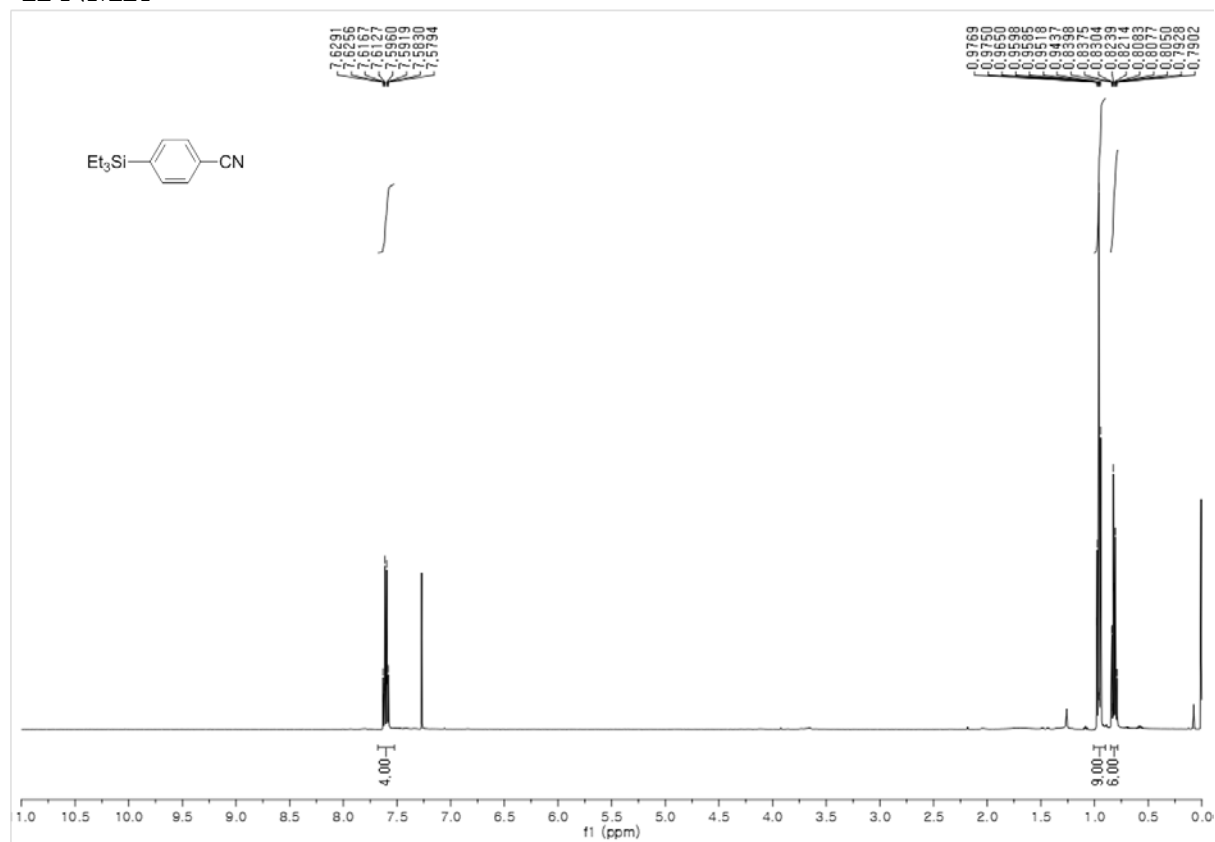
Triethyl(4-nitrophenyl)silane (2d)
 ^1H NMR



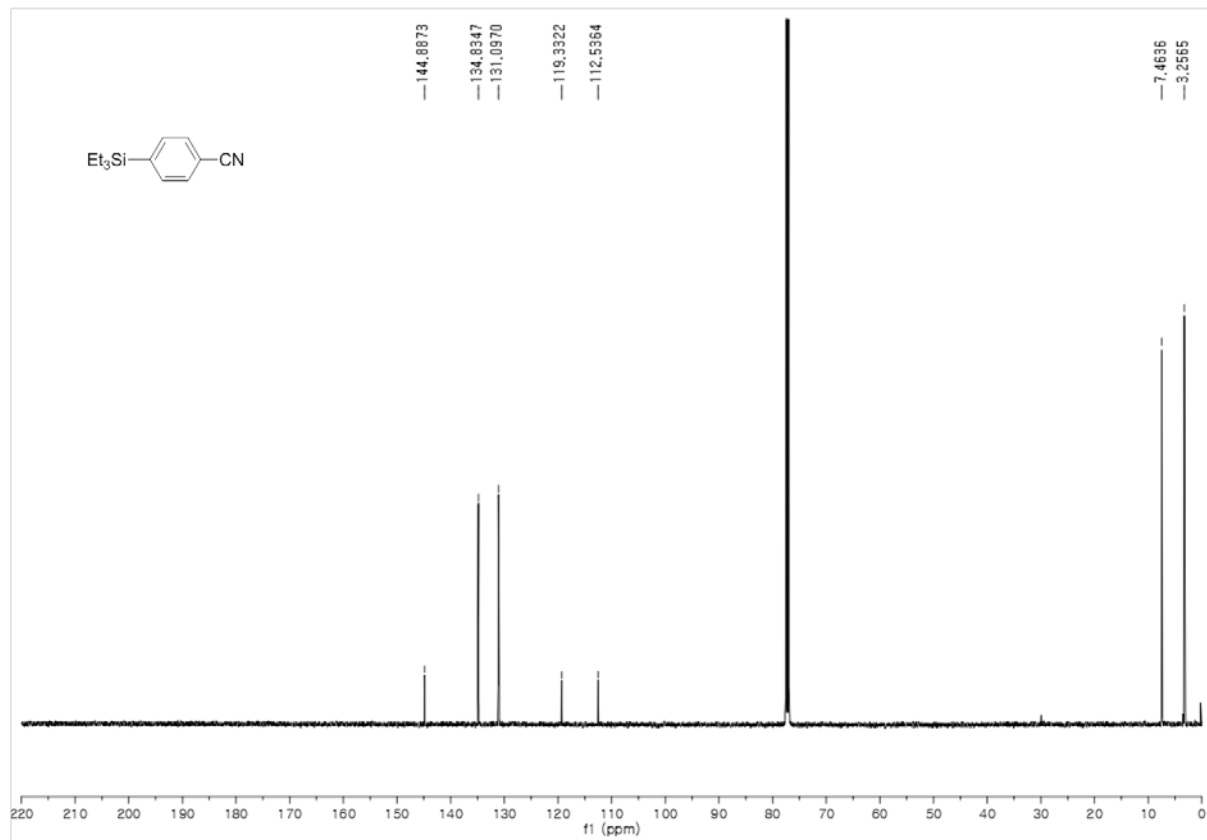
^{13}C NMR



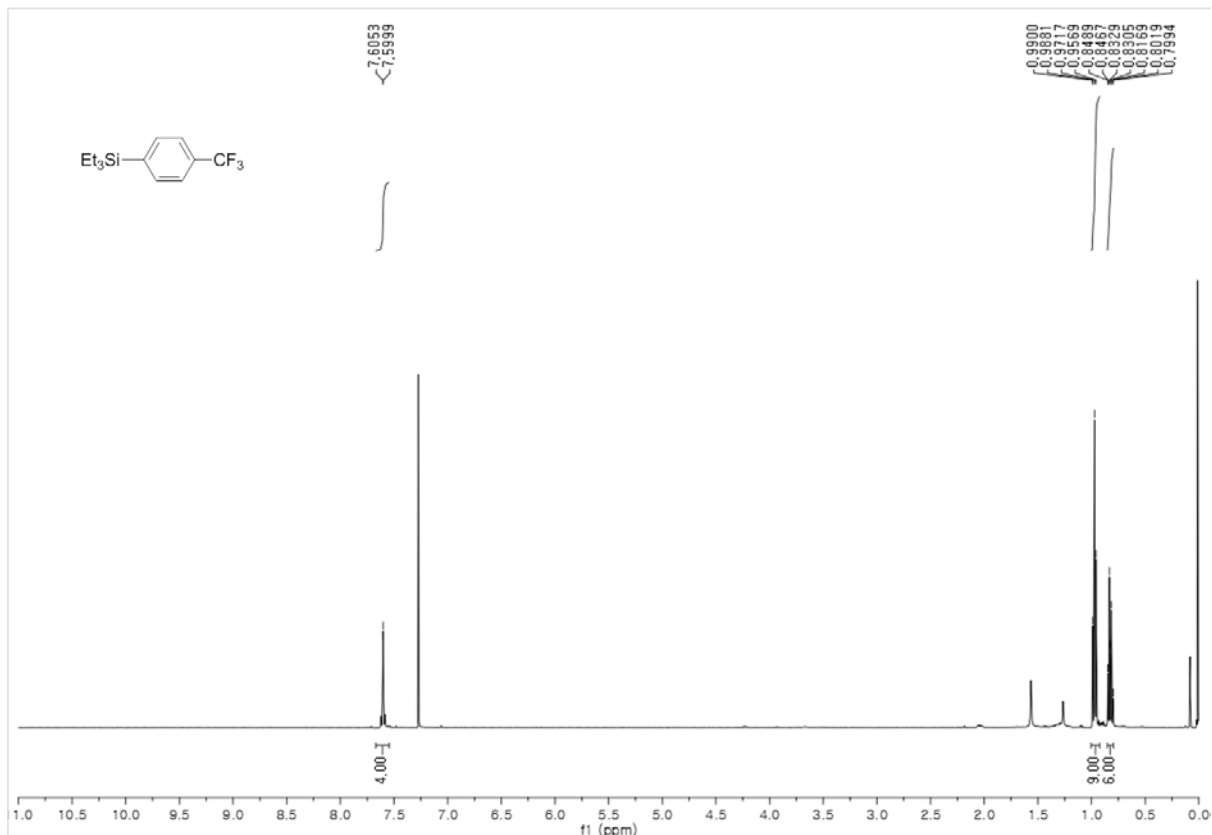
4-(Triethylsilyl)benzonitrile (2e)
 ^1H NMR



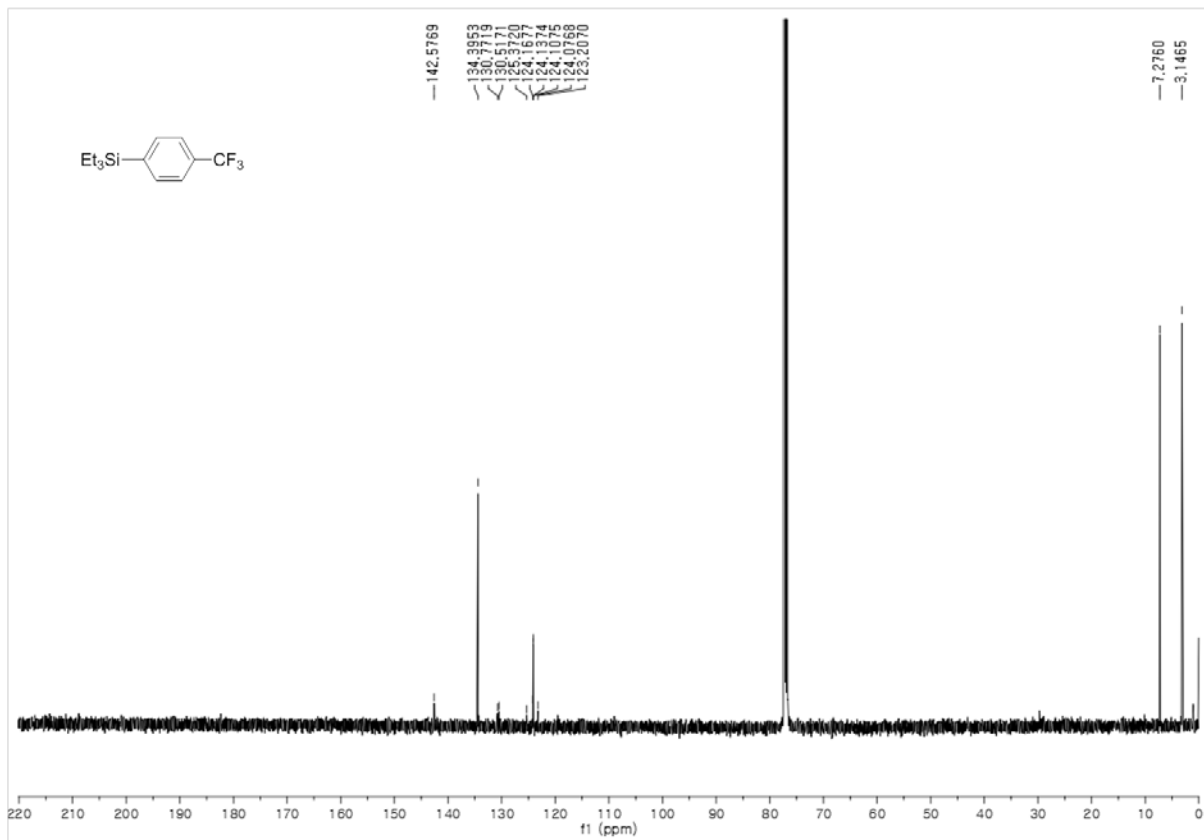
^{13}C NMR



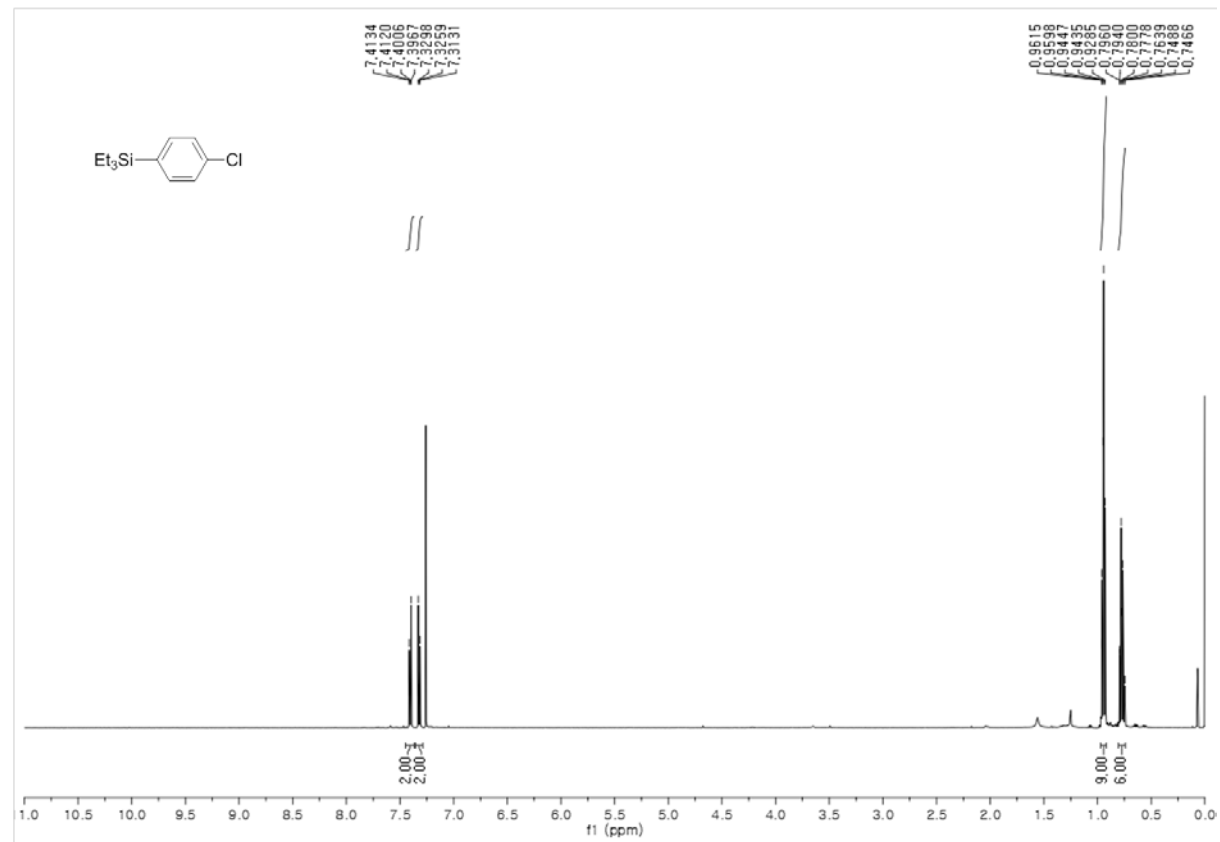
Triethyl(4-(trifluoromethyl)phenyl)silane (2f)
 ^1H NMR



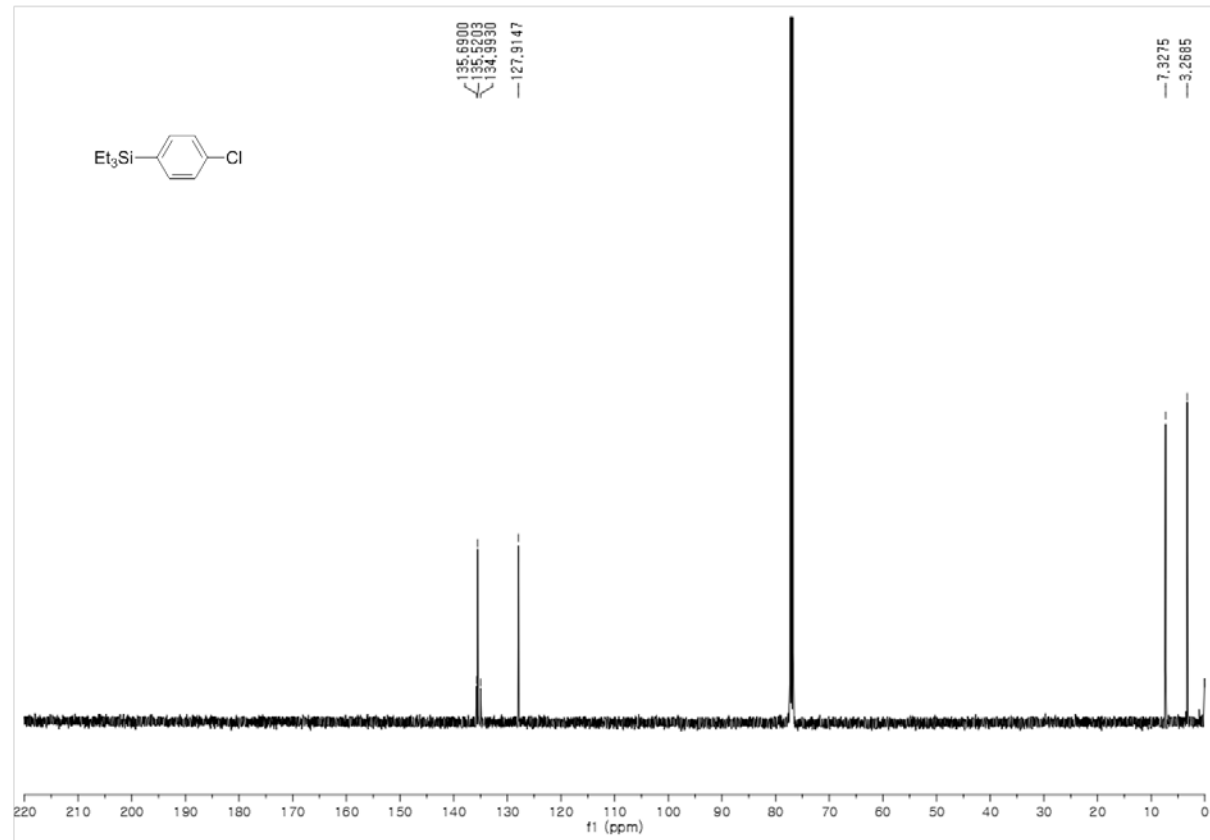
^{13}C NMR



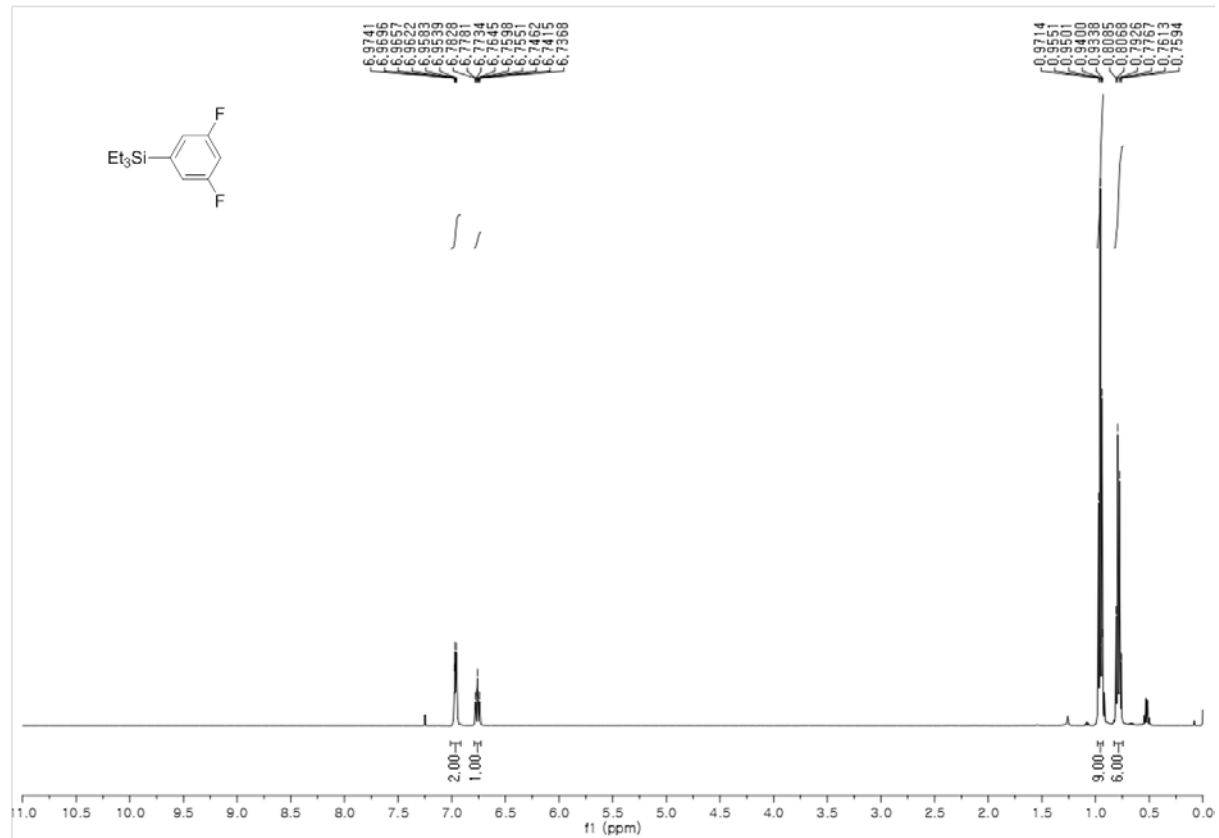
(4-Chlorophenyl)triethylsilane (2g)
¹H NMR



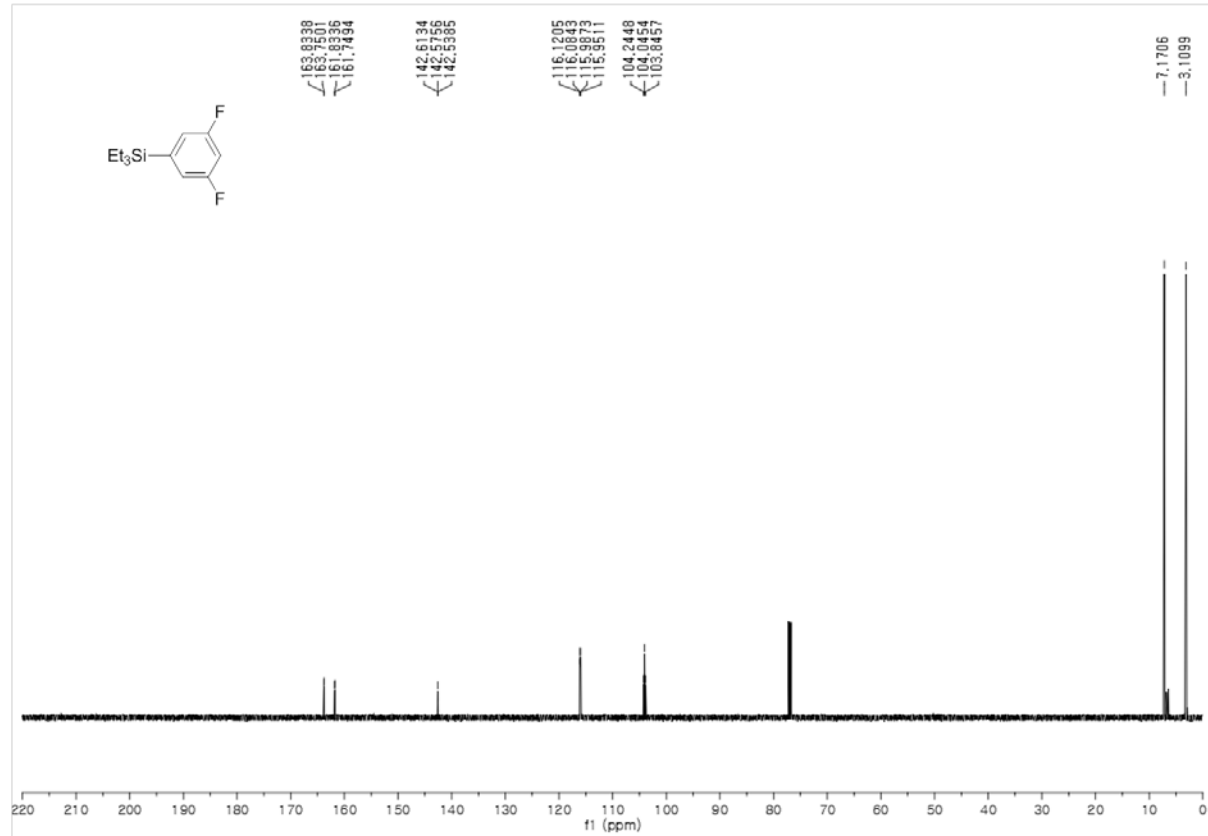
¹³C NMR



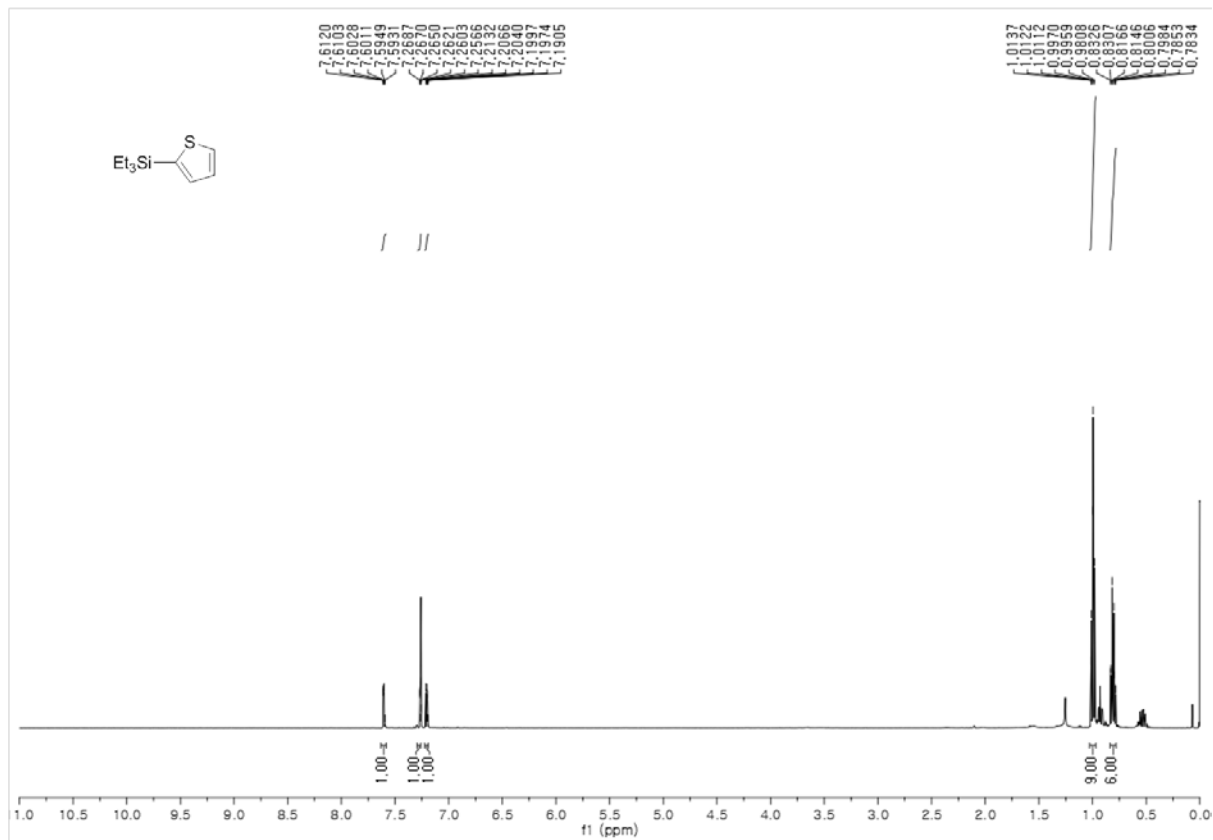
(3,5-difluorophenyl)triethylsilane (2h) ¹H NMR



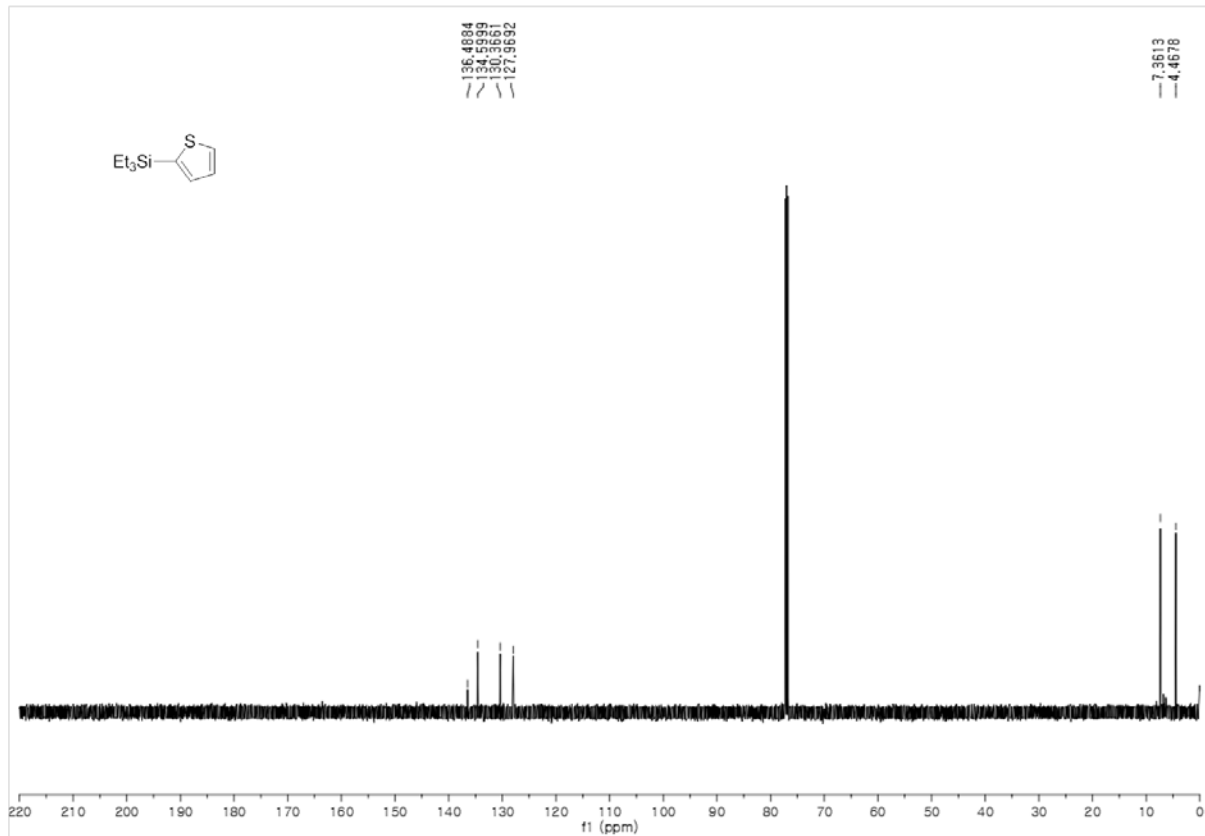
¹³C NMR



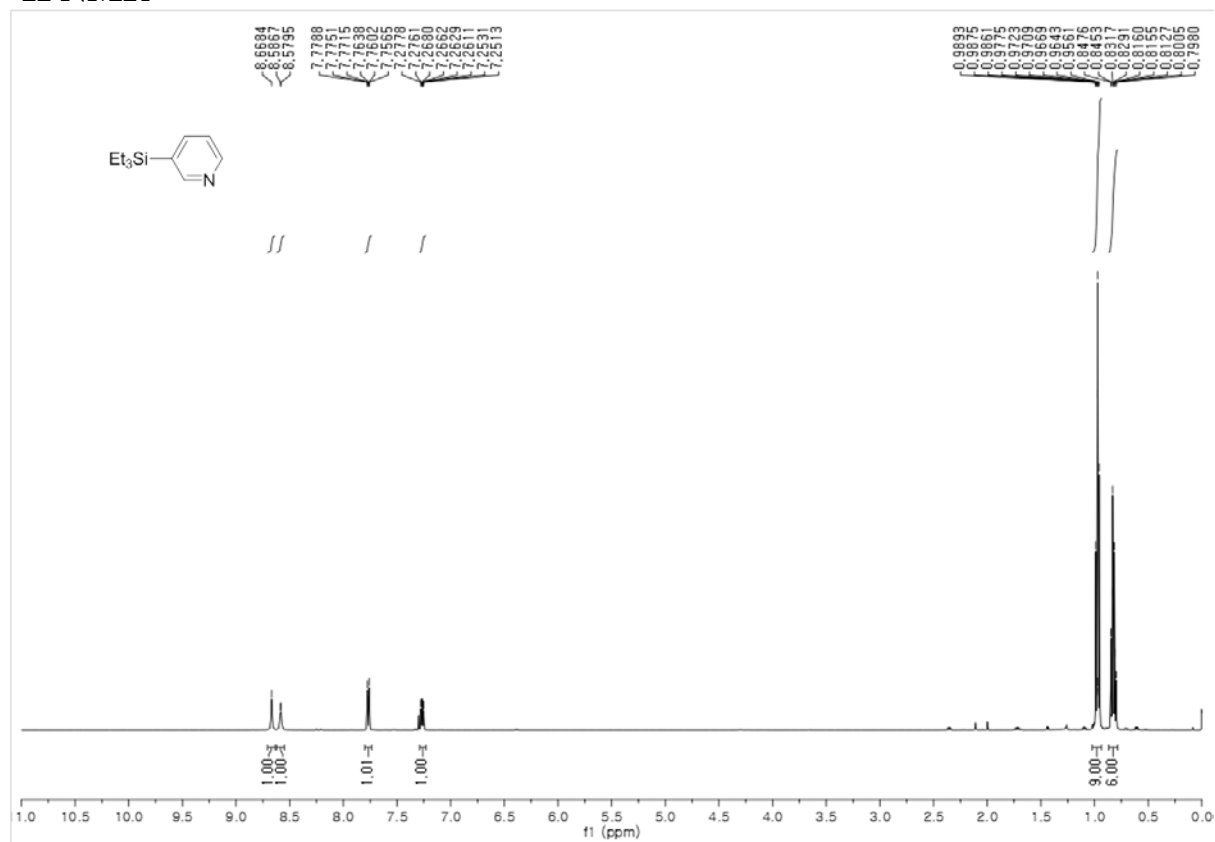
2-(Triethylsilyl)thiophene (2i)
 ^1H NMR



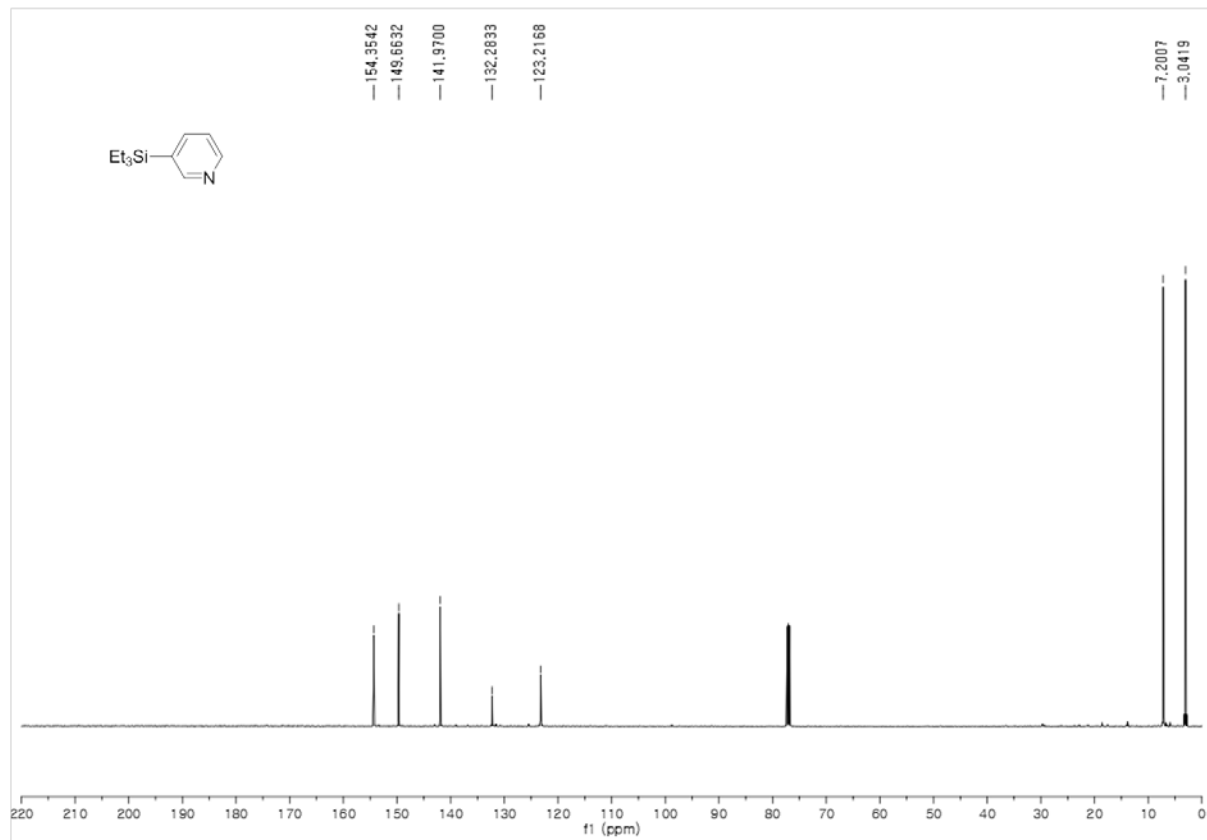
^{13}C NMR



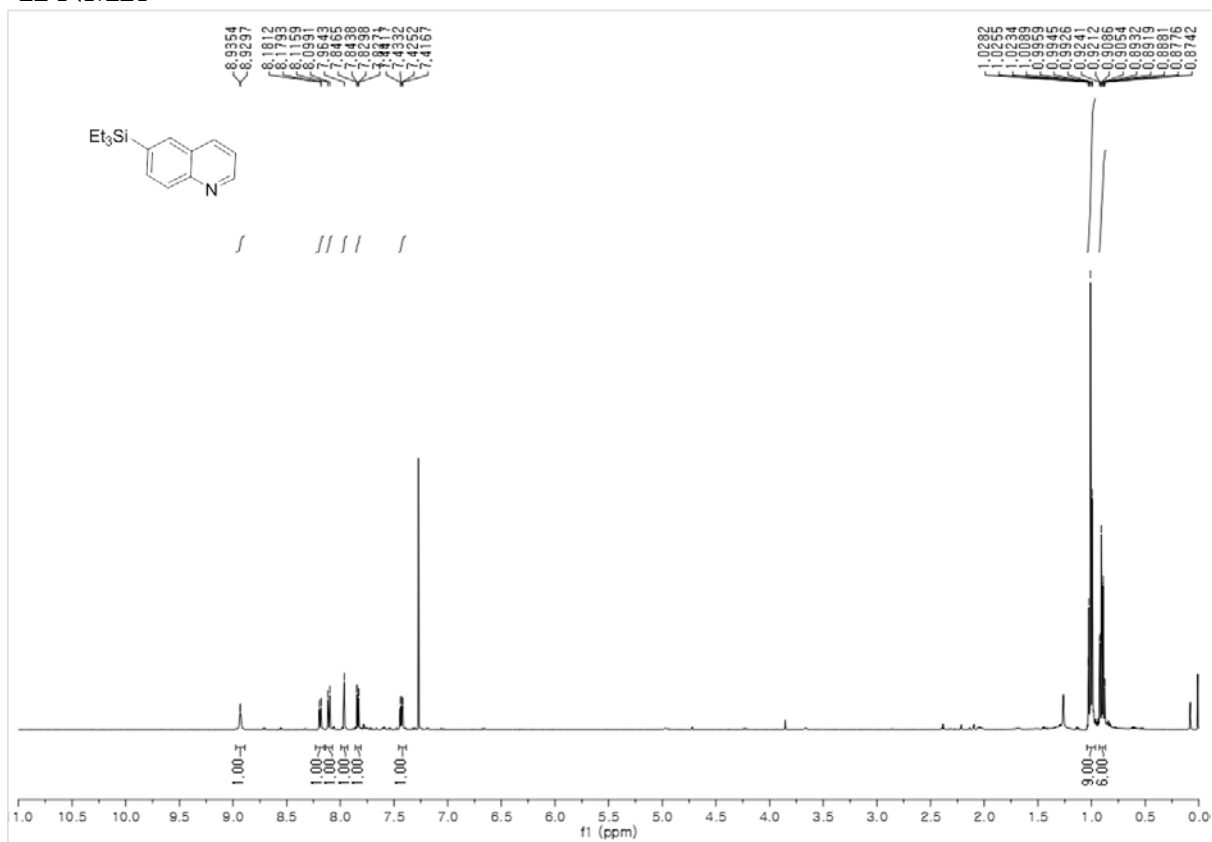
3-(Triethylsilyl)pyridine (2j)
 ^1H NMR



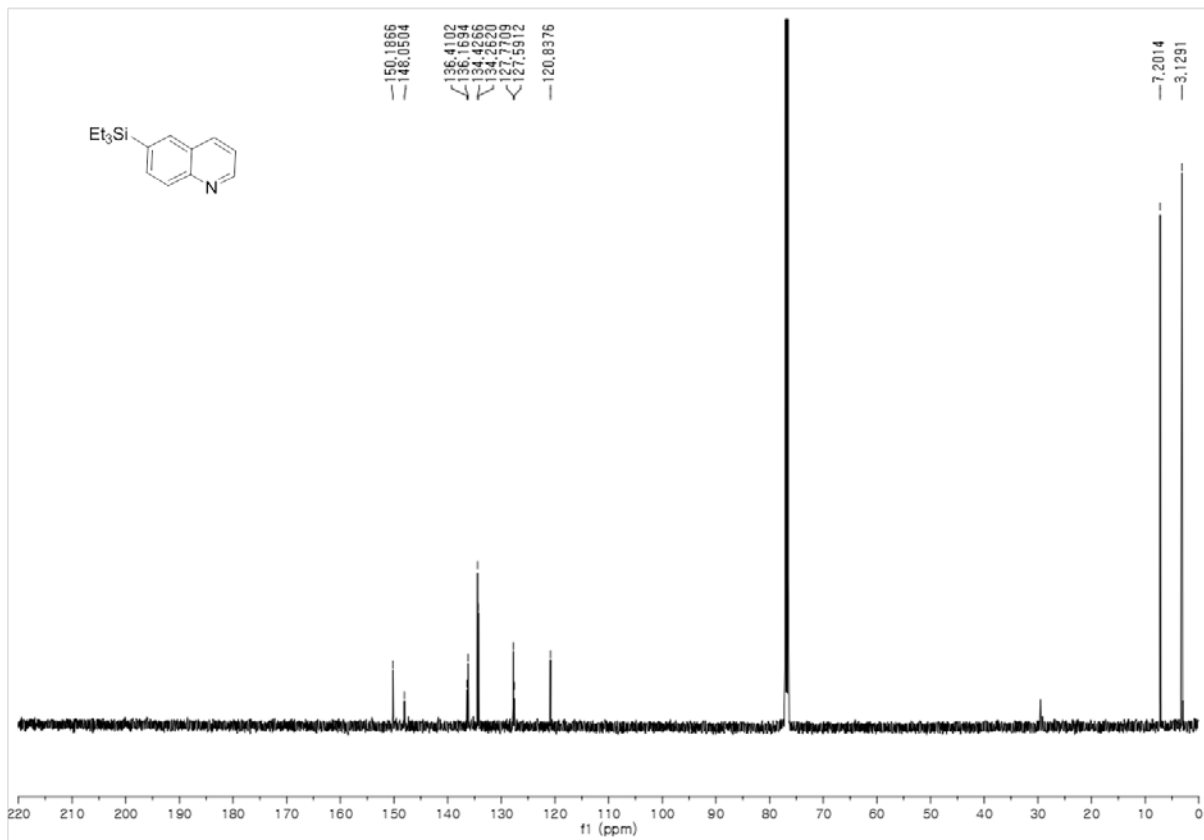
^{13}C NMR



6-(Triethylsilyl)quinoline (2k)
 ^1H NMR

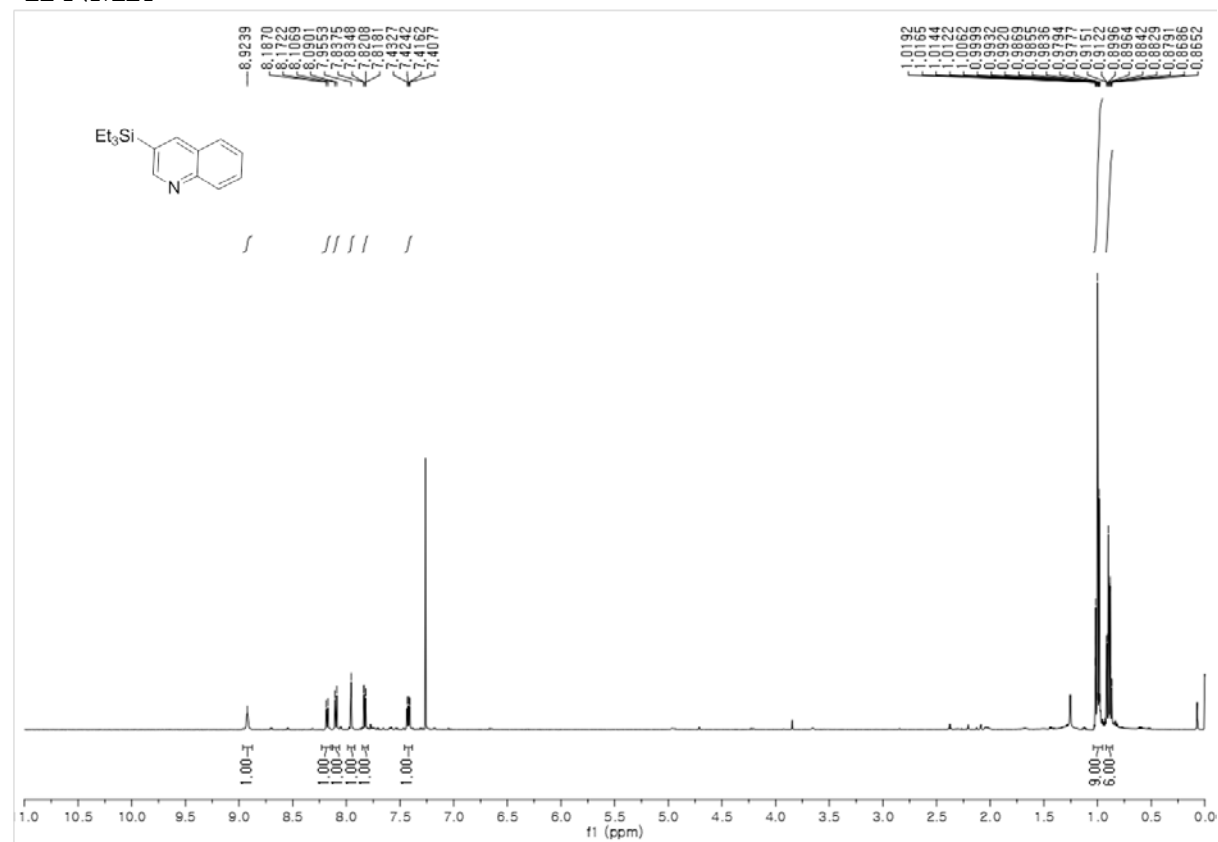


^{13}C NMR

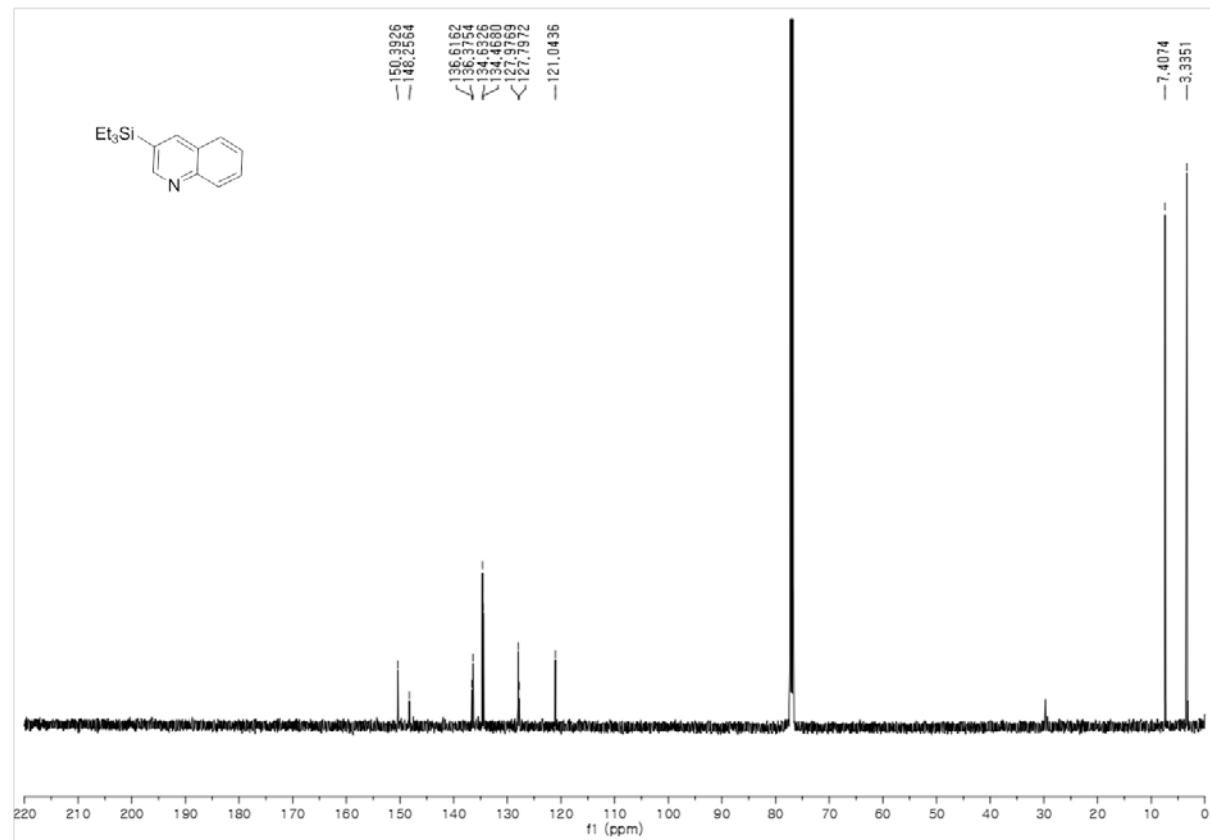


3-(Triethylsilyl)quinoline (2l)

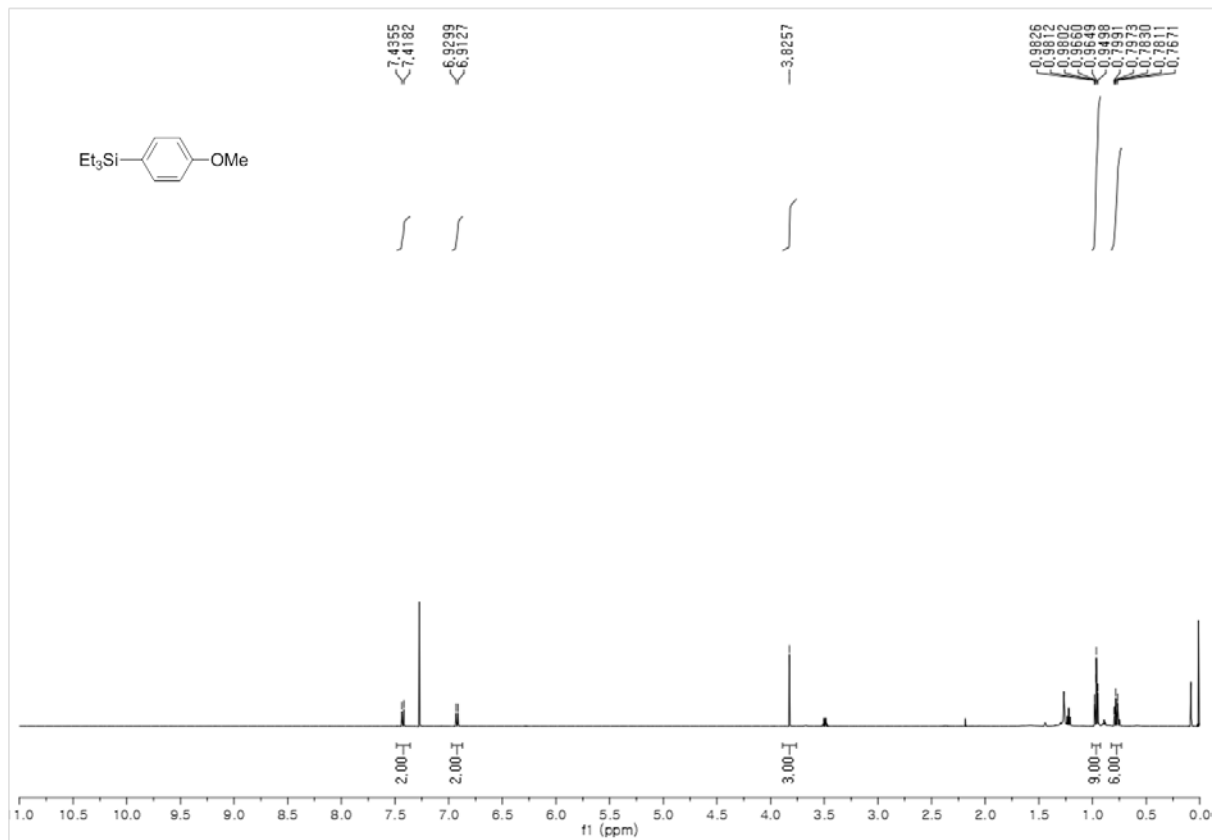
¹H NMR



13C NMR



Triethyl(4-methoxyphenyl)silane (2n)
 ^1H NMR



^{13}C NMR

